CRCLEME
Cooperative Research Centre for
Landscape Evolution & Mineral Exploration

OPEN FILE
REPORT
SERIES

CSIRO
EXPLORATION
AND MINING

AMIRA
Australian Mineral Industries Research Association Limited ACN 004 448 266

REGOLITH GEOLOGY AND GEOCHEMISTRY MT MAGNET DISTRICT

Geochemical orientation studies, Stellar and Quasar deposits

Volume 1

I.D.M. Robertson, J.D. King, R.R. Anand and C.R.M. Butt

CRC LEME OPEN FILE REPORT 92

March 2001

(CSIRO Division of Exploration and Mining Report 48C, 1994.
2nd Impression 2001.)

AMIRA
Australian Mineral Industries Research Association Limited ACN 004 448 266

CRCLEME
Cooperative Research Centre for
Landscape Evolution & Mineral Exploration

CSIRO
EXPLORATION
AND MINING

REGOLITH GEOLOGY AND GEOCHEMISTRY MT MAGNET DISTRICT

Geochemical orientation studies, Stellar and quasar deposits

Volume 1

I.D.M. Robertson, J.D. King, R.R. Anand and C.R.M. Butt

CRC LEME OPEN FILE REPORT 92

March 2001

(CSIRO Division of Exploration and Mining Report 48C, 1994.
2nd Impression 2001.)

CRC LEME is an unincorporated joint venture between The Australian National University, University of Canberra, Australian Geological Survey Organisation and CSIRO Exploration and Mining
Headquarters: CRC LEME c/o CSIRO Exploration and Mining, Private Bag No 5, PO Wembley, Western Australia, 6913.

RESEARCH ARISING FROM CSIRO/AMIRA YILGARN REGOLITH GEOCHEMISTRY PROJECTS 1987-1996

In 1987, CSIRO commenced a series of multi-client research projects in regolith geology and geochemistry which were sponsored by companies in the Australian mining industry, through the Australian Mineral Industries Research Association Limited (AMIRA). The initial research program, "Exploration for concealed gold deposits, Yilgarn Block, Western Australia" had the aim of developing improved geological, geochemical and geophysical methods for mineral exploration that would facilitate the location of blind, buried or deeply weathered gold deposits. The program commenced with the following projects:

P240: Laterite geochemistry for detecting concealed mineral deposits (1987-1991). Leader: Dr R.E. Smith.
Its scope was development of methods for sampling and interpretation of multi-element laterite geochemistry data and application of multi-element techniques to gold and polymetallic mineral exploration in weathered terrain. The project emphasised viewing laterite geochemical dispersion patterns in their regolith-landform context at local and district scales. It was supported by 30 companies.

P241: Gold and associated elements in the regolith - dispersion processes and implications for exploration (1987-1991). Leader: Dr C.R.M. Butt.
The project investigated the distribution of ore and indicator elements in the regolith. It included studies of the mineralogical and geochemical characteristics of weathered ore deposits and wall rocks, and the chemical controls on element dispersion and concentration during regolith evolution. This was to increase the effectiveness of geochemical exploration in weathered terrain through improved understanding of weathering processes. It was supported by 26 companies.

These projects represented 'an opportunity for the mineral industry to participate in a multi-disciplinary program of geoscience research aimed at developing new geological, geochemical and geophysical methods for exploration in deeply weathered Archaean terrains'. This initiative recognised the unique opportunities, created by exploration and open-cut mining, to conduct detailed studies of the weathered zone, with particular emphasis on the near-surface expression of gold mineralisation. The skills of existing and specially recruited research staff from the Floreat Park and North Ryde laboratories (of the then Divisions of Minerals and Geochemistry, and Mineral Physics and Mineralogy, subsequently Exploration Geoscience and later Exploration and Mining) were integrated to form a task force with expertise in geology, mineralogy, geochemistry and geophysics. Several staff participated in more than one project. Following completion of the original projects, two continuation projects were developed.

P240A: Geochemical exploration in complex lateritic environments of the Yilgarn Craton, Western Australia (1991-1993). Leaders: Drs R.E. Smith and R.R. Anand.
The approach of viewing geochemical dispersion within a well-controlled and well-understood regolith-landform and bedrock framework at detailed and district scales continued. In this extension, focus was particularly on areas of transported cover and on more complex lateritic environments typified by the Kalgoorlie regional study. This was supported by 17 companies.

P241A: Gold and associated elements in the regolith - dispersion processes and implications for exploration (1991-1993). Leader: Dr. C.R.M. Butt.
The significance of gold mobilisation under present-day conditions, particularly the important relationship with pedogenic carbonate, was investigated further. In addition, attention was focussed on the recognition of primary lithologies from their weathered equivalents. This project was supported by 14 companies.

Most reports related to the above research projects were published as CRC LEME Open File Reports Series (Nos 1-74), with an index (Report 75), by June 1999. Publication now continues with release of reports from further projects.

P252: Geochemical exploration for platinum group elements in weathered terrain. Leader: Dr C.R.M. Butt.
This project was designed to gather information on the geochemical behaviour of the platinum group elements under weathering conditions using both laboratory and field studies, to determine their dispersion in the regolith and to apply this to concepts for use in exploration. The research was commenced in 1988 by CSIRO Exploration Geoscience and the University of Wales (Cardiff). The Final Report was completed in December 1992. It was supported by 9 companies.

P409: Geochemical exploration in areas of transported overburden, Yilgarn Craton and environs, WA.
Leaders: Drs C.R.M. Butt and R.E. Smith.
About 50% or more of prospective terrain in the Yilgarn is obscured by substantial thicknesses of transported overburden that varies in age from Permian to Recent. Some of this cover has undergone substantial weathering. Exploration problems in these covered areas were the focus of Project 409. The research was commenced in June 1993 by CSIRO Exploration and Mining but was subsequently incorporated into the activities of CRC LEME in July 1995 and was concluded in July 1996. It was supported by 22 companies.

Although the confidentiality periods of Projects P252 and P409 expired in 1994 and 1998, respectively, the reports have not been released previously. CRC LEME acknowledges the Australian Mineral Industries Research Association and CSIRO Division of Exploration and Mining for authority to publish these reports. It is intended that publication of the reports will be a substantial additional factor in transferring technology to aid the Australian mineral industry.

This report (CRC LEME Open File Report 92) is a second impression (second printing) of CSIRO, Division of Exploration and Mining Restricted Report 48C, first issued in 1994, which formed part of the CSIRO/AMIRA Project P409.

Copies of this publication can be obtained from:
The Publication Officer, c/- CRC LEME, CSIRO Exploration and Mining, Private Bag 5, Wembley, WA 6913, Australia. Information on other publications in this series may be obtained from the above or from http://leme.anu.edu.au/
Cataloguing-in-Publication:

Regolith geology and geochemistry Mt Magnet District - Geochemical orientation studies, Stellar and Quasar deposits.
ISBN v1: 0 643 06682 9 v2: 0 643 06683 7 set: 0 643 06684 5
1. Regolith- Western Australia 2. Gold ores - Western Australia 3. Geochemistry - Western Australia 4. Geology - Western Australia
I. Robertson, I.D.M. II. Title
CRC LEME Open File Report 92.
ISSN 1329-4768

PREFACE AND EXECUTIVE SUMMARY

The CSIRO-AMIRA Project "Exploration in Areas of Transported Overburden, Yilgarn Craton and Environs" (Project 409) has, as its principal objective, development of geochemical methods for mineral exploration in areas with substantial transported overburden, through investigations of the processes of geochemical dispersion from concealed mineralization. The Project has two main themes. One of these, *'Surface and subsurface expression of concealed mineral deposits'* is addressed by this report, which focuses on the Stellar and Quasar mines in the Boogardie Synform at Mt. Magnet.

A wide variety of sedimentary materials comprise the transported cover in the Yilgarn Craton. The most widespread is a colluvium of heterogeneous gravels with a fine grained matrix, derived from partial stripping of a lateritic regolith. The colluvium overlies older sediments and/or a complete or partly truncated lateritic regolith. This situation prevails in the depositional plains overlying the Boogardie Synform. The colluvium is derived from stripping of the lateritic profile, including banded iron formations, that outcrop around the synform. The colluvium generally directly overlies a lateritic profile, developed on felsic and mafic-ultramafic rocks. This profile has been truncated at Quasar and partly truncated at Stellar. Palaeochannels, below the colluvium, infilled with dominantly sandy and argillaceous sediments, are important features at both sites. Since deposition, precipitations of silica, to form hardpan, secondary carbonates and, locally, smectites have occurred. The whole sequence is a testimony to the complex history and evolution of the landforms and regolith.

The problems confronting exploration at Mt. Magnet are typical of many well-mineralized districts in the Yilgarn Craton, namely:-

1. A heterogeneous, multiphase cover of essentially exotic sediments that has no initial geochemical or mineralogical relationship with the underlying rocks.
2. A deeply weathered basement, hosting mineralization.
3. Areas lacking widespread, buried lateritic residuum so that the uppermost weathered basement may either be leached of gold or, even if not, presents a small target.
4. Difficulties in distinguishing between transported and residual regolith, particularly in drill cuttings.
5. A high background Au abundance in the colluvium (approximately 50 ppb), due to its derivation from a highly mineralized region, masks any subtle anomalies due to post-depositional hydromorphic dispersion from concealed mineralization.

The geochemical orientation studies at Stellar and Quasar were based on multi-element analyses of drill samples, regolith mapping, drill logging and inspection of mine exposures. Although only a few drill holes were available at Stellar, special drilling at Quasar provided detailed coverage around and over the deposit. There appears to have been a pronounced Au-As anomaly in clay-rich lateritic duricrust at Stellar, although its extent could not be established. There was also a sub-horizontal, supergene enrichment "blanket" at the base of the overburden, but this was mined before research commenced. In contrast, at Quasar, where the profile is truncated, there is no prominent geochemical dispersion halo from the mineralization in either the residual or transported components of the regolith. Investigation of element distributions in various regolith horizons reveals only equivocal dispersion haloes for gold, with the most promise shown by interface sampling that incorporates the unconformity between colluvium and basement. This procedure has little value where palaeochannels are present. At both sites, most element distribution patterns in the saprolite relate to basement lithology, with good contrasts between felsic and mafic/ultramafic parent rocks. In the sediments, the abundances suggest a mixture, dominated by more mafic lithologies, with any spatial variations reflecting either overburden type (*e.g.* colluvium or palaeochannel clays) or provenance. Mineralization at both sites is poor in pathfinder elements, hence a multi-element solution to the interpretation of total Au distribution in the high-background of the colluvium is not readily achieved. However, elevated abundances of Bi, Pb and Zn may be related to the occurrence of mineralization at Quasar and an additive index using these elements, with or without Au, appears to improve target sizes at the colluvium/bedrock interface.

This orientation study has demonstrated the need for careful regolith mapping and establishing regolith stratigraphy, and precise, well-controlled geochemical analysis as essential prerequisites for data interpretation in these complex environments. These requirements become more acute when specialised techniques, such as sampling of specific regolith components, selective extractions or manipulation of data from particular horizons become necessary.

C.R.M. Butt and R.E. Smith
Project Leaders.

29th July 1994.

CONTENTS

		Page
1	ABSTRACT	4
2	INTRODUCTION	5
	2.1 Location, access, climate and vegetation	5
	2.2 Exploration history	5
	2.3 Exploration problems	5
	2.4 Objectives	7
	2.5 CSIRO work program	7
3	STUDY METHODS	7
	3.1 Lag sampling	7
	3.2 Drillhole sampling	7
	3.2.1 Quasar	7
	3.2.2 Stellar	9
	3.3 Petrography	9
	3.4 XRD mineralogy	9
	3.5 Geochemical analysis - WMC	9
	3.6 Data verification	9
	3.7 Data presentation	10
4	REGIONAL AND LOCAL GEOLOGY	11
	4.1 Regional geology	11
	4.2 Local geology - Quasar Deposit	11
	4.3 Local geology - Stellar deposit	12
5	REGOLITH-LANDFORM RELATIONSHIPS	12
	5.1 Introduction	12
	5.2 Regional distribution	12
	5.2.1 Erosional regimes	12
	5.2.2 Depositional regimes	15
6	REGOLITH STRATIGRAPHY, CHARACTER AND PALAEOTOPOGRAPHY	16
	6.1 Stellar	16
	6.1.1 Basement	16
	6.1.2 Palaeochannel sediments	29
	6.1.3 Colluvium-alluvium	30
	6.2 Quasar	31
	6.2.1 Basement	31
	6.2.2 Palaeochannel sediments	31
	6.2.3 Colluvium-alluvium	31
7	GEOCHEMISTRY	33
	7.1 Background and threshold abundances	33
	7.2 Dispersion in section	34
	7.2.1 Stellar	34
	7.2.2 Quasar	35

Page

7.3 Dispersion in plan 37
7.3.1 Top of saprolite and saprolite-colluvium interface 37
7.3.2 Palaeochannel sediments 45
7.3.3 Colluvium-alluvium 49
7.3.4 Lag 50
7.4 Regolith discrimination 50
7.4.1 Stellar 50
7.4.2 Quasar 52

8 SUMMARY AND CONCLUSIONS 54
8.1 Regolith-landform evolution 54
8.1.1 Laterite 54
8.1.2 Transported overburden 55
8.2 Three dimensional regolith modeling 55
8.3 Geochemistry 56
8.3.1 Geochemical data verification 56
8.3.2 Geochemical backgrounds and thresholds 56
8.3.3 Pathfinder elements 56
8.3.4 Geochemical distinction of regolith units and bedrock lithology 56
8.3.5 Top of basement sampling 57
8.3.6 Interface sampling 57
8.3.7 Palaeochannel sediment 58
8.3.8 Colluvium-alluvium 58
8.3.9 Lag 58
8.4 Implications for Exploration 58
8.5 Recommendations for further research 59

9 ACKNOWLEDGEMENTS 60

10 REFERENCES 60

APPENDICES Volume II

1 ABSTRACT

Recent exploration under the lag-strewn colluvium-alluvium covered plain, mantling the Boogardie Synform, has located concealed Au mineralisation at Stellar and Quasar. The area is difficult to explore due to structural complexity in the basement, high geochemical backgrounds from numerous mineralised settings, a variably stripped, residual regolith beneath the transported overburden and scattered, high Au contents in the overburden. Pit exposures at Stellar and drilling at Quasar also revealed palaeochannel sediments hidden beneath the colluvium.

Regolith-landform relationships in the district were established by mapping the regolith of an area of 25 km^2 around the mines and inspecting drill cuttings and pit exposures. A palaeochannel, filled with mega-mottled, grey clay and sandy clay, with some sepiolite towards the top and detrital, ferruginous, lateritic nodules, pisoliths and authigenic black granules towards the base, is exposed at Stellar. At Quasar, a similar palaeochannel occurs south-west of the pit and was detected by drilling. These fluvial channels appear to have been incised in already weathered basement and the sediments themselves have undergone post-depositional weathering. At Stellar, a clay-rich lateritic duricrust has formed by the weathering and later cementation of a partly transported unit overlying both the felsic and mafic-ultramafic bedrocks. Contemporary weathering of clays in the palaeochannel was probably responsible for the development of mega-mottles and some ferruginous granules. The colluvial-alluvial overburden was derived from dismantling the lateritic regolith. It contains lateritic nodules and pisoliths, probably from a proximal source, but is dominated by polymictic fragments, including BIF, ferruginous saprolite and saprolite, set in a silty-clay matrix. Its upper 2-3 m is silicified to red-brown hardpan.

Analytical data for a suite of 24 elements was provided by Hill 50 NL; the Ti and Zr data were unreliable and not used. Although geochemical backgrounds and thresholds have been established for the major regolith units, these must be regarded as of local application only because no data from distant background areas was available. Elevated concentrations of Cr, Ni, Cu, V and, possibly, Zn indicate mafic-ultramafic rocks. The saprolite and mottled zone have a significantly greater Cr/Fe ratio than the transported materials. Although the laterite has a high Cr/Fe ratio, Cr and Ni were ineffective for discriminating between laterites developed over felsic and mafic-ultramafic rocks. Regolith differentiation can be improved by canonical analysis; the most useful elements appear to be Al, Fe, Ni, Cr, Ga, Y, Zn, Th and Cu.

The Au mineralisation is poor in pathfinder elements such as As and Sb but there are weak anomalies in Bi and Pb. There is no correlation between the composition of the basement and the overlying colluvium, nor between nearly adjacent layers within the colluvium and its overlying lag. Unless partial extraction geochemistry can indicate basement-related anomalies in the colluvium-alluvium, this blanket must be penetrated to reach the weathered Archaean beneath. Comparison of sampling the top of the basement with that of the unconformity, or interface, between basement and colluvium, indicates lower order but broader and more consistent anomalies in the interface; this can be improved using additive indices of Bi, Pb and Zn. The interface sample is, therefore, the preferred sample medium, in this area of buried, stripped regolith, except where there are palaeochannels. Where there has been less regolith stripping and a buried laterite occurs, as at Stellar, this is the preferred sample medium.

2 INTRODUCTION

2.1 Location, access, climate and vegetation

Mount Magnet is located 560 km NNE of Perth, in the Murchison Province of the Yilgarn Craton. The Stellar and Quasar Au deposits lie some 5 km to the west, within the Boogardie Synform. Access to the deposits from Mt Magnet is by a sealed part of the Boogardie Station road and, within mining leases, by gravel roads and exploration tracks.

The Mount Magnet district has a semi-arid to arid climate, with a recorded average annual rainfall of 234 mm. Rainfall variability is high and results mostly from frontal systems from the west and south-west in winter and from patchy, convectional storms and cyclone-related rain-bearing depressions in summer. Summers generally are dry and hot to very hot; winters are cool to mild, with a few frosts. The vegetation is dominated by mulga (Accacia spp) and by various types of poverty bush and turpentine (Eremophila spp), with isolated kurrajong trees on depositional surfaces.

2.2 Exploration history

Recent exploration within the largely colluvium-covered core of the Boogardie Synform (Figure 1) has continued since the early 1980's and has been conducted by Carpentaria Exploration Co. Ltd., Renison Goldfields Consolidated Ltd., (RGC), Metana Minerals N.L. Pty., Ltd, and Western Mining Corporation Ltd., (WMC) as Hill 50 Gold Mine NL. The Stellar and Quasar Au deposits, discovered by RGC and Metana respectively in 1989, represent new discoveries and are the first 'blind' orebodies to be mined by Hill 50 Gold Mines within the synform.

Although outcrop in the synform core is sparse, potential host lithologies (ultramafic schists and intrusive dacitic quartz porphyry) were recognised in bedrock exposures within Jones Creek, and in the enclosing outcropping units (e.g., BIF) of the Sirdar Formation (Marjoribanks, 1989). Mineralised structures, e.g., the Hill 50 and Hesperus Dawn faults, which host significant mineralisation elsewhere, extend through the synform and intersect these lithologies; the area was considered highly prospective (Vann, 1989; Perriam, 1990).

Systematic rotary air blast (RAB) drilling was used by RGC, through the transported cover, to recognisable bedrock to target Fe-rich, geochemically responsive horizons, e.g., buried laterites and mottled zones (Gatehouse, 1989). This led to the discovery of mineralisation at Stellar, Milky Way, Boomer and Andromeda. The Quasar mineralisation was discovered by bedrock reconnaissance drilling by Metana Minerals.

2.3 Exploration problems

There are three significant exploration problems within the core of the Boogardie Synform:-

i) As in much of the Yilgarn Craton, the area has been subjected to deep lateritic weathering during the Tertiary (Butt and Smith, 1980). Buried remnants of complete, or nearly complete, deeply weathered profiles occur within the central area. Where present, these upper, ferruginous horizons are excellent geochemical sample media. Elsewhere, because of erosion of the ferruginous horizons, the buried profiles are partly stripped and the uppermost residual component, commonly saprolite, may be depleted in Au and pathfinder elements.

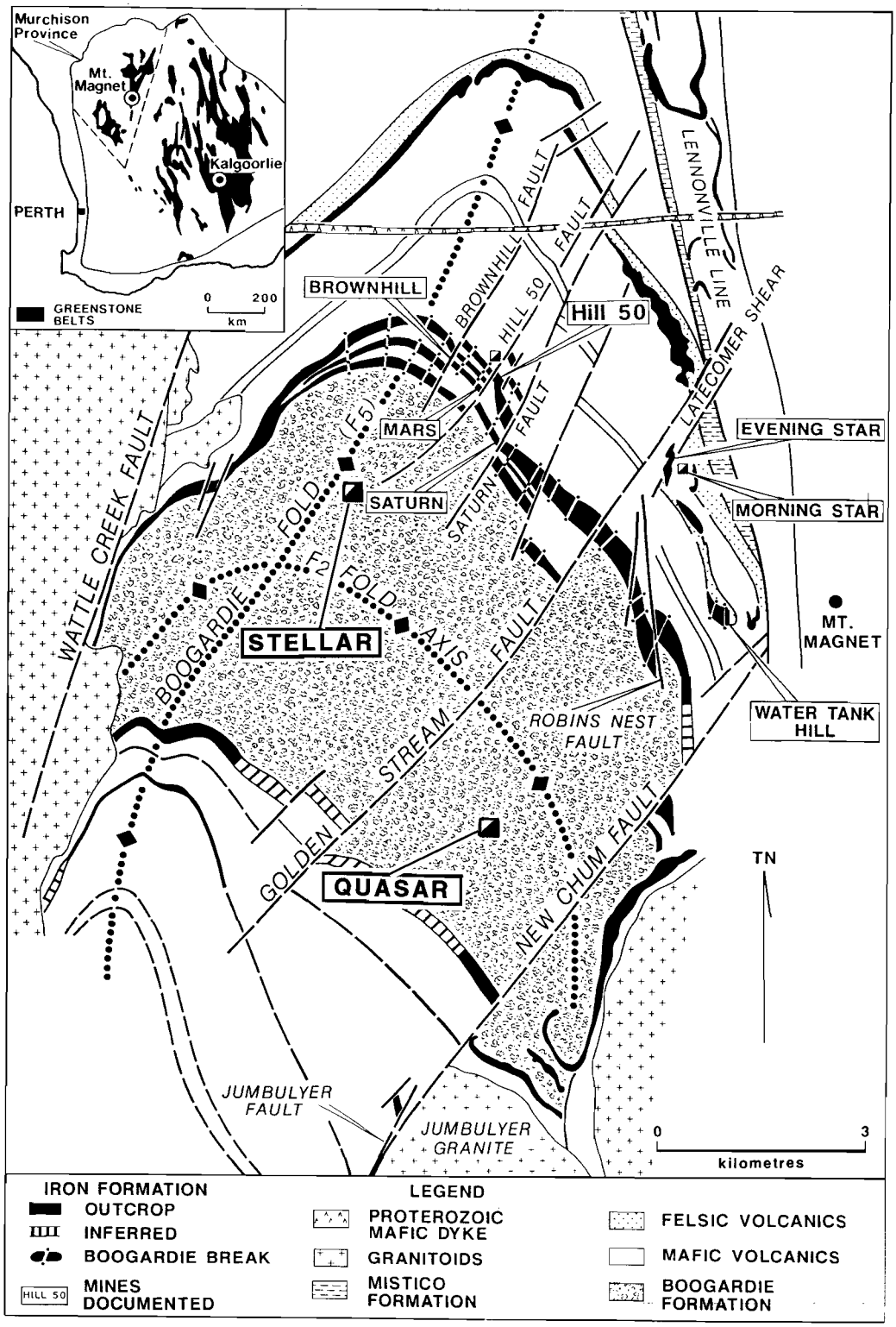

Figure 1. Geological map of the Mt Magnet Area after Thompson *et al.*, (1990). See Section 4 for description of geology.

ii) Structural complexity, and the variety and large number of mineralised settings in the synform core, has made it difficult to establish geochemical thresholds and backgrounds satisfactorily. Consequently, subtle geochemical anomalies, representing mineralisation, are difficult to distinguish within these locally high backgrounds.

iii) Most of the area is covered by locally-derived Tertiary to Recent colluvium-alluvium, strewn with a polymictic lag of lateritic and lithic materials, including BIF fragments. The BIF fragments and the lateritic debris are both potentially auriferous and tend to mask geochemical signatures from underlying rocks. Consequently, the total element geochemistry of surficial sediments is probably unreliable, even at a district scale.

2.4 Objectives

The objective of this study was to investigate the dispersion of gold and associated elements in the regolith about the Stellar and Quasar deposits, with a view to identifying the optimum sample media and analytical suite for continuing exploration of the Mt Magnet district.

This was to be achieved by regolith-landform mapping in the vicinity of the deposits, logging drill cuttings from the Stellar and Quasar deposits, examining and mapping regolith exposures in the Stellar and Quasar pits and selecting material from drill cuttings and pit faces for major and trace element analysis and petrographic examination at CSIRO. The remainder of the study was to involve interpretation of element distributions with respect to regolith characteristics and relationships to mineralisation, with a view to optimising geochemical exploration procedures.

2.5 CSIRO work program

Research by CSIRO has comprised studies of the surface geology and geomorphology, the geochemistry of surface materials and the geochemistry of, and dispersion in, the regolith, particularly within the sediments. The study has been based largely on orientation drill sampling by Hill 50 Gold Mine NL, who also supplied most of the geochemical data (Appendices Q1 and S1). Pit exposures were examined and sampled during early visits to the area but, during the tenure of the investigation, little pit exposure, at Stellar, was directly accessible, for safety reasons.

3 STUDY METHODS

3.1 Lag sampling

All lag sampling was by Hill 50 Gold Mine NL, after the drilling had been completed, but prior to the commencement of this study. The 2-6 mm fraction was collected. Samples were taken as closely as possible to the drill sites, attempting, where possible, to find undisturbed ground. The lag samples were not washed prior to analysis.

3.2 Drillhole sampling

Bags of RAB drill cuttings were transferred to sample farms by Hill 50 Gold Mine NL prior to mining and were accessible for sampling and logging. Each was spear-sampled by Hill 50 Gold Mine NL.

3.2.1 Quasar

One hundred and twenty five holes were drilled on a regular grid and the cuttings made available for this orientation study. One hundred holes were logged and samples from 57 were submitted for multi-element analysis. Holes were selected for analysis on the basis of their availability and their location; whether proximal to the mineralization or distant from it for establishing

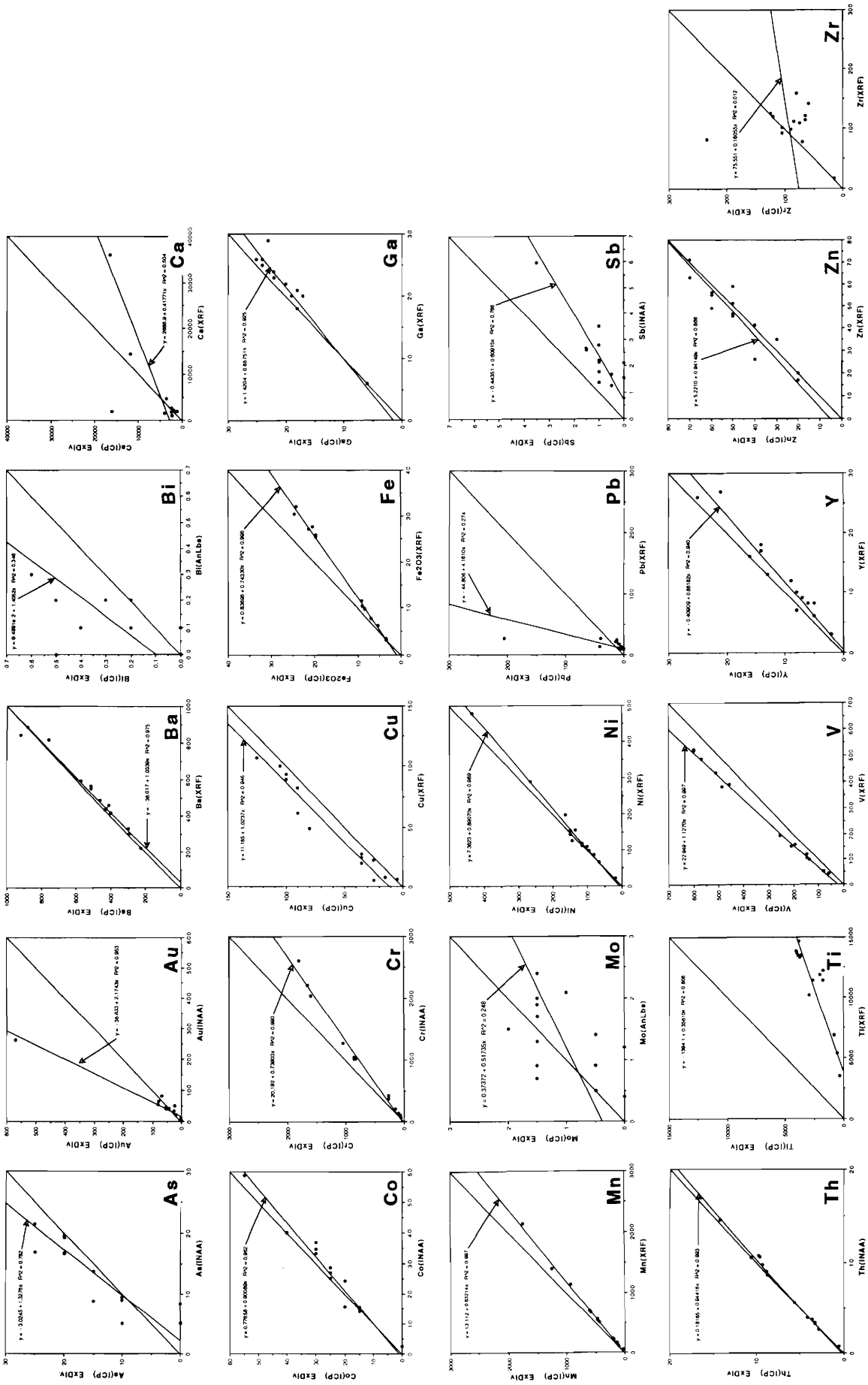

Figure 2. Scattergrams of WMC Exploration Divivision Laboratory ICP data against CSIRO XRF and Becquerel INAA data.

background. Where possible, an approximately equidimensional grid was sampled to facilitate data presentation.

3.2.2 Stellar

Forty two drillholes, on two separate grids, were logged. Of these, seven holes, on an approximately east-west section, which represent the main lithological and regolith units, were sampled for multi-element analysis. Bags of drill cuttings from the remainder, covering a north-south section, had not been properly labelled and could not be reliably identified after transport by Hill 50 Gold Mine NL from the drill-site to the sample farm; these were not investigated further.

3.3 Petrography

Large specimens of regolith materials, collected from the pits and their surroundings, were impregnated with resin, cut by diamond saw and rough-polished prior to examination by binocular microscope under oblique illumination. Smaller specimens were selected from these and polished mounts were prepared for microscopic examination under oblique and normally reflected light.

3.4 XRD Mineralogy

Pulped samples were examined by CuKα radiation, using a Philips PW1050 diffractometer, fitted with a graphite crystal diffracted beam monochromator. Each sample was scanned over a range 3-65° 2θ at a speed of 1° 2θ/min and data were collected at 0.02° 2θ intervals. Charts, plotted at 0.5° 2θ/cm were used for interpretation.

3.5 Geochemical Analysis - WMC

The lag and drill samples were submitted for analysis to WMC's Exploration Division Laboratory. All samples were oven dried and jaw-crushed to <6 mm. The samples were riffle split to a 100 g aliquot, which was milled in Cr steel to 90% <75 µm, prior to analysis. A suite of 24 elements (Ag, As, Au, Ba, Bi, Ca, Co, Cr, Cu, Fe, Ga, Mn, Mo, Nb, Ni, Pb, Sb, Th, Ti, U, V, Y, Zn and Zr) was analysed using a triple acid digest ($HF/HNO_3/HClO_4$) and read by ICP. In addition, the samples from Stellar were also analysed for Al and Si by ICP. Detection limits were as follows (in ppm unless stated otherwise):- Fe (0.1%); Ca (0.01%); Zn, V (10); Cr, Mn, Co, Ni, Cu, As, Ba, Ti, Zr, Ga (5); Pb (2); Nb, Y (1); Ag, Sb, Mo (0.5); Bi, Th, U (0.1); Au (0.001).

3.6 Data verification

A suite of 14 samples from Quasar, previously analysed by WMC, were submitted for analysis by XRF (CSIRO), by INAA (Becquerel Laboratories) and by ICPMS (Analabs). Samples were selected from mineralised and unmineralised drillholes QGI39, QGI61, QGI59, QGI57 and QGI81 (see Figure 10) to represent as broad a suite of trace elements and major elemental matrices as possible.

INAA

Thirty gramme aliquots were encapsulated at CSIRO and sent to Becquerel Laboratories for INAA analysis. Detection limits were as follows (in ppm unless stated otherwise):- K (0.2%); Fe (500); Zn, Ba, Na (100); Rb (20); Ag, Se, Cr, Mo (5); W, Ce, Br, U (2); As, Co, Cs, Ta (1); La, Eu, Yb, Hf, Th (0.5); Sb, Sm, Lu (0.2); Sc (0.1); Ir (0.02); Au (0.005).

XRF

X-ray fluorescence analysis was performed at CSIRO on fused discs (0.7 g sample and 6.4 g Li borate) using a Philips PW1480 instrument by the method of Norrish and Hutton. Detection limits were as follows (in ppm unless stated otherwise):- Si, Al (0.01%); Mg, Na (0.01%); Fe (0.005%); Ti (0.003%); Mn, P (0.002%); Ca, K (0.001%); Ba (30); Ce, Cl (20); Cr, Co, Cu, La, Ni, S (10); Pb, Rb, Sr, V, Y, Zn, Zr (5); Nb (4); Ga (3).

ICPMS

ICPMS analysis was performed by Analabs (Perth). Prior to analysis, the samples were digested in HNO_3/HCl/$HClO_4$/HF (Method GS201). Detection limits were as follows (in ppm):- Ni, Pb (2), Mo, Ag, Bi (0.1).

A comparison between the highly reliable data from INAA analysis and the XRF data (Appendix G2) indicates close agreement for Fe, Ni, Cr, and Pb in terms of correlation (r^2=0.998-0.982) and slope (1.04-0.88). Intercepts were small (<= detection limit). There was a little more scatter for Ba. The Co data showed significant scatter, particularly among Fe-rich samples, indicating that a correction for the Fe-rich matrix had not been optimally applied to the XRF data. If these Fe-rich samples were removed, the regression improved significantly. The verification data are given in Appendix G1.

The best of these data were then compared with that supplied by Hill 50 Gold Mine NL (Figure 2). Good correlations and slopes were obtained for Ba, Co, Cu, Ga, Ni, Th, Y, V and Zn. Moderately good correlations were obtained for Cr, Fe, Mn, Ti, and Sb but all these Hill 50 Gold Mine NL data were low (slopes 0.74-0.36) (Figure 2). This probably reflects an incomplete dissolution or poor calibration. Moderate to poor correlations were shown by Bi, Au and As, for which the results were consistently high. The Au data show an artificially high correlation due to one outlier. If this outlier was removed, the slope improved considerably. This Au-rich sample may have been nuggety. Particularly poor results were obtained for Ca, Mo, Ti and Zr (Figure 2). The poor Ca and Mo results reflect low abundances; the poor Zr and Ti results seem to reflect incomplete dissolution of some samples which is to be expected, considering the method. These results were discarded from the database and have not been considered further. Good accuracy and precision for Ti and Zr are essential where these are to be used individually and as a ratio in rock type discrimination. Where consistently low results were obtained (e.g., Fe and Cr), the results of these comparisons need to be considered and, where necessary, corrected for when interpreting the data.

3.7 Data presentation

The data distribution in plan view was adequate for contouring of specific sample horizons or depth intervals. The data for each area were gridded at a 15 x 15 m mesh, using a moving weighted least squares method (weighting exponent 2.0), utilising the nearest 8 points. The weighted values were used to compute a first order polynomial for each grid node. This method was chosen as it closely honours the control points. Difficulty was encountered with highly variable and skewed data (e.g., Au) which, in the untransformed form, produced contoured anomalies that were larger than implied by the point data. Log(10) transforms were applied and the data translated during contouring, to produce a more accurate result. Contours were smoothed using four filtering passes. Contour intervals were chosen to display the data with maximum sensitivity but minimum clutter. Thresholds and higher values are shown with a heavier line (Appendix Q7). Where the distribution of data did not adequately fill a rectangular area, the contoured product has been clipped to indicate the limits of confidence.

All plans and sections refer to the metric Hill 50 grid. In some places (e.g., Stellar) there are no less than three grids, because of the complex exploration history.

4 REGIONAL AND LOCAL GEOLOGY

4.1 Regional geology

The Mount Magnet greenstone belt comprises ultramafic, mafic, and felsic volcanic rocks, with subordinate sediments, banded iron formation (BIF) and chert. The sequence is intruded by minor felsic and mafic rocks and is surrounded by batholiths and stocks of variably deformed gneissic granitoids (Archibald, 1982; Watkins and Hickman, 1990). The regional structure and stratigraphy have been established by Watkins and Hickman (1990) and Thompson *et al.*, (1990). There are several important differences in the interpretation of the geological structure and stratigraphy but that of Thompson *et al.*, (1990), revised by Perriam (1990), is locally in use and has been adopted here. The sequence has been complexly deformed into a major domal structure, with a steeply plunging, synformal configuration, the Boogardie Synform (Figure 1). The synform is broad, open, with a NNE-trending axial plane and north closure, about which all the rocks of the sequence are disposed (Marjoribanks, 1989). Major faulting is evident on both east and west margins of the belt, on the Mount Magnet Fault Zone and the Wattle Creek Shear Zone respectively. Local faulting parallels the axis of the synform and is dominantly sinistral (Balde and Woolfe, 1990).

Facing information in the synform core is limited. Thompson *et al.*, (1990) report that, in the southern parts, the facing direction is to the south whereas, in the north, facings are to the north, indicative of a complex structure. In the study area, from the base upwards, the stratigraphic units are :-

Boogardie Formation: This comprises talc-carbonate altered ultramafic flows of originally olivine peridotite, with other MgO-rich mafic rocks. The sequence is cut by fine- to medium-grained felsic intrusives.

Sirdar Formation: This hosts the majority of exposed mineralisation in the Hill 50 mine area. It consists of four banded iron formations, known as the 'Saturn Bars' with intercalated mafic volcanic flows that are overlain by a spinifex-textured ultramafic flow and by a thin sequence of felsic flows and tuffs (Thompson *et al.*, 1990). The Saturn Bars outline the hinge and the eastern limb of the Boogardie Synform. The lowermost bar separates the Sirdar from the Boogardie Formation.

Cover: Most of the Archaean rocks of the Boogardie Synform are obscured by a cover of colluvium-alluvium, in part underlain by palaeochannels. The thickness of the colluvial-alluvial cover is variable and generally thickens away from the enclosing BIF ridges. Bedrock exposures in the synform interior are restricted to the incised drainage of Jones Creek.

4.2 Local geology - Quasar deposit

Gold mineralization is associated with a ductile shear zone, developed in talc-chlorite-sericite altered, high-MgO mafic-ultramafic rocks, at the structural contact with a felsic-porphyry stock. The mineralisation is poor in sulphides and quartz veining. Weakly mineralised quartz-tourmaline veining is restricted to the felsic porphyry, occurring marginal to the contact.

The bedrock is overlain by about five metres of hardpanised colluvium-alluvium. A palaeochannel, predating the colluvial-alluvial sediments, lies to the east of the pit area and consists of white kaolinitic clays with layers of lateritic nodules and pisoliths. The colluvial-alluvial and palaeochannel cover, described in detail in Sections 6.2.2 and 6.2.3, overlies weakly mottled, clay-rich saprolite, silicified over some felsic-porphyry. The base of oxidation on the

mafic-ultramafic rocks is around 35 m; on the felsic rocks the depth of weathering is variable, from a few metres to >40 m near the sheared contact.

4.3 Local geology - Stellar deposit

Gold mineralization is associated with quartz-tourmaline veining in a brittle, dilational zone and is hosted by dacitic quartz porphyry, near its structural contact with an ultramafic rock. The mineralisation is sulphide poor. The Archaean rocks, exposed in the pit, have been weathered to various felsic and mafic-ultramafic saprolites, in part overlain by lateritic duricrust. The residual profile is partly truncated by a palaeochannel, filled with mottled, puggy clays and is overlain by colluvium-alluvium. These are described in detail in Sections 6.1.2 and 6.1.3.

5 REGOLITH-LANDFORM RELATIONSHIPS

5.1 Introduction

The Mt. Magnet area is an integral part of the array of deeply-weathered terrain of the Yilgarn Craton. Geochemical dispersion in such terrain is best interpreted in terms of the evolution of the landforms and regolith. This has been established by mapping the regolith of a 5 x 5 km area, encompassing both Quasar and Stellar at 1:25 000 (Figure 3). The regolith stratigraphy and the characteristics of the regolith were determined from inspection of drill cuttings and mine exposures and this has formed the basis for an understanding of regolith history, dispersion patterns and for preliminary 3-dimensional modeling of the regolith around both mines.

5.2 Regolith distribution

Mapping identified several regolith-landform units that are related to the deeply weathered mantle and to its modification by erosional and depositional processes (Figure 3). A schematic cross section, showing regolith-landform relationships for the mapped area, is shown in Figure 4. Using the classifications *residual, erosional* and *depositional* regimes, the mapped area is mantled by erosional and depositional regimes. The terminology used here, for regolith-landform mapping units, is given in detail by Anand *et al.*, (1993).

5.2.1 Erosional regimes

Erosional regimes, as defined, are those areas where erosion has removed the lateritic residuum to the level where ferruginous saprolite, saprolite or fresh rock are either exposed or concealed beneath modern soils or a veneer of locally-derived sediments. Erosional regimes cover about 25% of the mapped area and are largely restricted to areas of relief associated with outcropping BIFs. Pediments to the BIF ridges form gentle slopes, mantled by acidic, red earths and are blanketed by a coarse lag of BIF fragments, vein quartz, lateritic nodules, pisoliths and ferruginous saprolite. Some BIF crops out within these pediments. This erosional regime may be subdivided into three mappable units, EBR3, ESP4 and ESP2.

Unit EBR3 forms the dominant relief of the Boogardie Synform and consists of outcropping, semi-continuous, BIF strike ridges. In places, for example north of Stellar, the BIFs are deeply weathered and lateritised.

Unit ESP4 is developed on truncated, weathered profiles of bedrock, and forms generally concave upland slopes, flanking the BIF ridges. These slopes are covered by a thin, red, largely residual soil, mantled by a coarse lag, dominated by fragments of BIF and vein quartz. Bedrock commonly crops out near the ridge top but becomes progressively buried down slope, giving way to a depositional regime. Regolith materials are commonly saprolitic and, in some places, ferruginous.

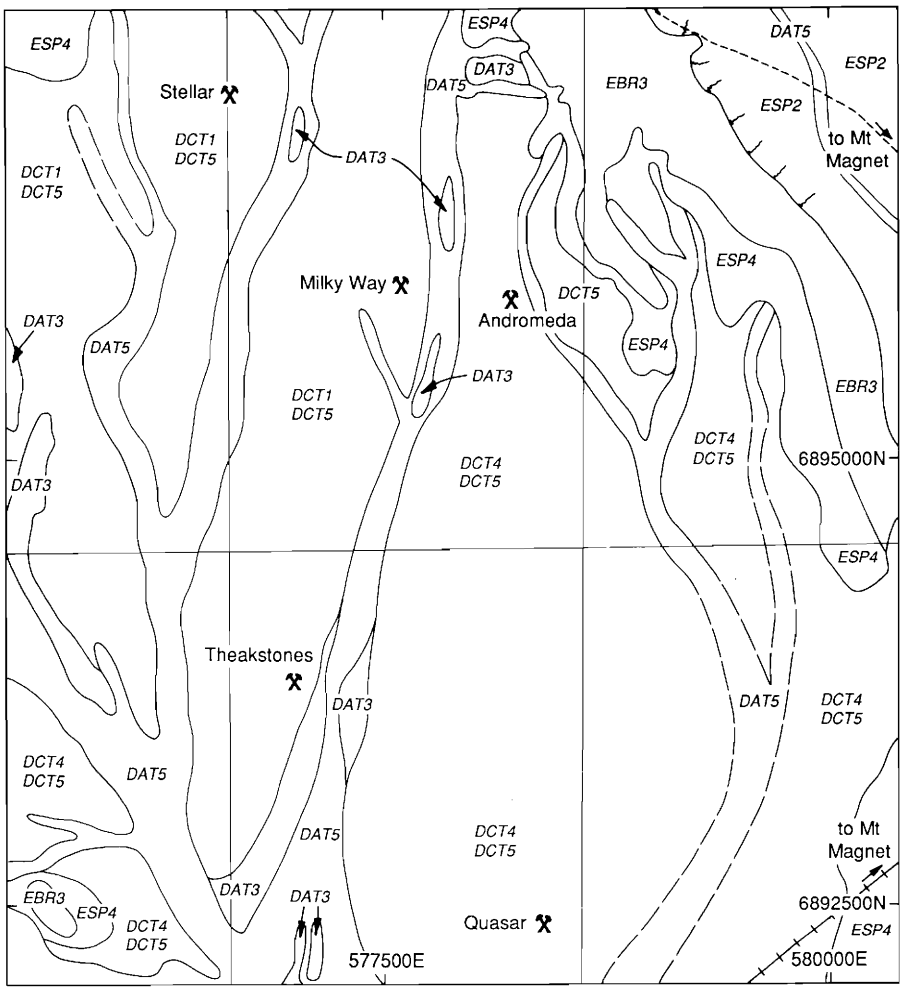

Figure 3. Regolith map of the Mt Magnet area.

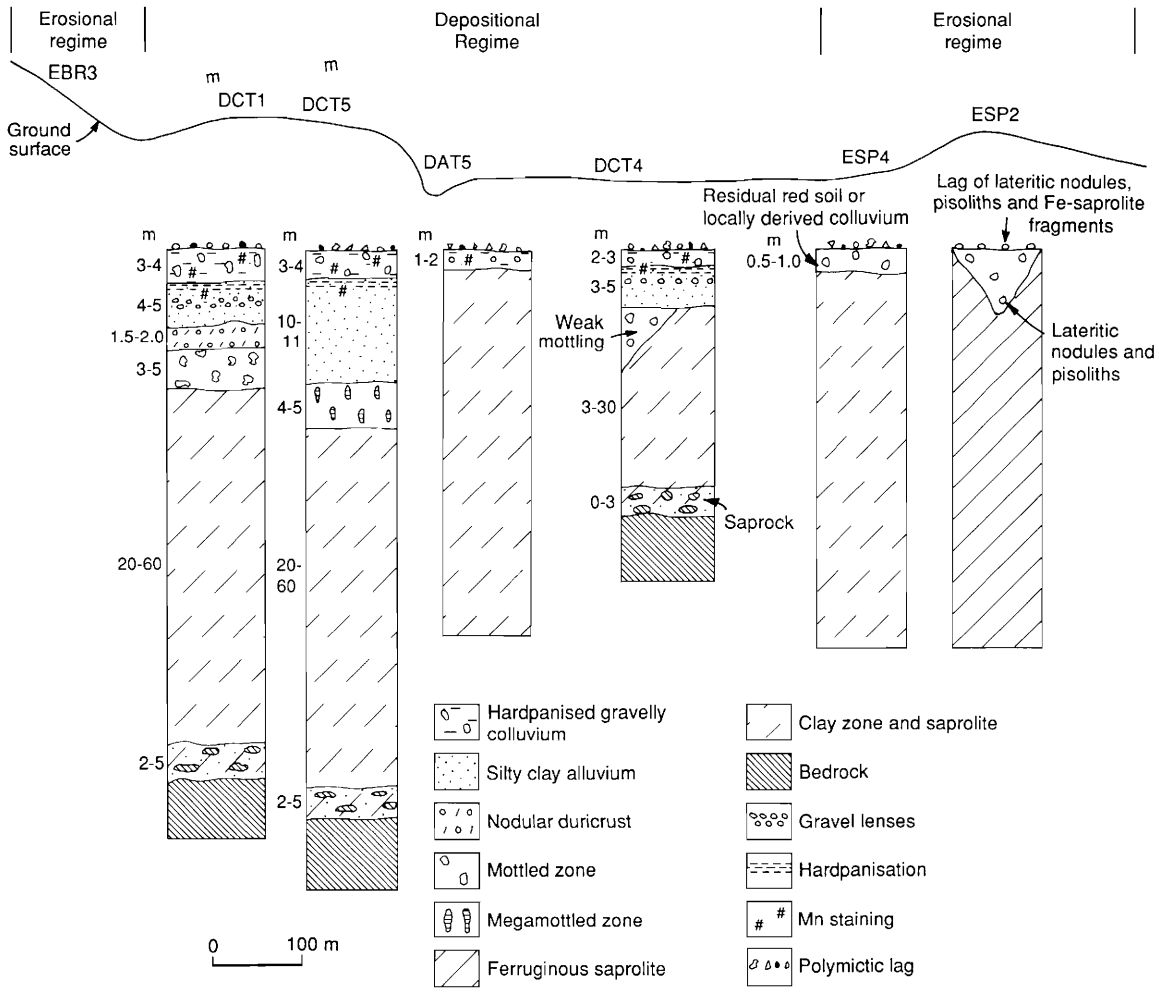

Figure 4. Generalised regolith-landform relationships for the mapped area (see Figure 3).

Unit ESP2 occurs in the north-east corner of the study area and is represented by breakaway escarpments, developed on the northern margin of the enclosing BIF ridges. Erosion has exposed ferruginous saprolite on the upper, breakaway surface and clay-rich or ferruginous saprolite on the lower surface. Both surfaces are mantled by fragments of BIF, derived from up slope, and a thin, residual soil. Scattered patches of lateritic duricrust are preserved on the upper breakaway surface. Tubular structures, up to one metre wide, are widely distributed across the erosional surface. These were voids that have been infilled with lateritic nodules and pisoliths and possibly represent relic tree root structures. The lower surface becomes progressively buried by recent sediments, up to one metre thick, but is still considered to be erosional.

5.2.2 Depositional regimes

Depositional regimes cover the lower slopes and the colluvial-alluvial plains and form widespread regolith-landform units that occupy about 75% of the mapped area (Figure 2). Their surfaces are strewn with polymictic lag. An extensive colluvial-alluvial blanket covers both complete and variably truncated lateritic profiles. The provenances of these sediments range from local to distal and thicknesses reach 20 m. Concealed beneath this colluvial-alluvial cover are earlier depositional regimes, consisting of mottled, clay-rich and lateritic materials, confined to palaeochannels. There are four mappable units within these depositional regimes (Figure 4).

Unit DAT5 is represented by active, modern drainage within the synform, dominated by the south-flowing Jones Creek. The drainage either rests on a hardpanised substrate of red-brown, silty clay, with interbedded gravel lenses or, as in Jones Creek, it has incised the hardpanised cover, exposing the underlying rocks.

Unit DAT3 forms overbank deposits along major drainages. The unit is apparent on the air-photos and has formed where high-volume, high-velocity, water flow has breached confining levees and stripped the levee banks of vegetation and lag. The unit is dominated by up to two metres of hardpanised cover, as described for Unit DAT5, resting on ferruginous saprolite or a saprolitic substrate.

Unit DCT4, DCT5, best exposed in the Quasar Pit, forms the dominant regolith type within the study area. It occurs as outwash plains down slope of units ESP4 and EBR3, mainly east of Jones Creek. It consists of a mixed colluvial-alluvial cover, generally less than eight metres thick, comprising polymictic gravels of lateritic nodules, pisoliths, lithic fragments and gravel lenses in a red-brown, clay-silt matrix. The upper five metres are commonly hardpanised to a variable depth. The sediments overlie a truncated, residual weathered profile, generally saprolite on ultramafic rocks and clay-saprolite on felsic rocks. The upper, ferruginous, lateritic zone is absent, with only scattered patches of weakly ferruginous saprolite remaining. Near Quasar, infilled palaeochannels increase the total thickness of transported cover to 14 m; thin dolomitic horizons have developed in these palaeochannels.

Unit DCT1, DCT5 occurs as outwash plains, mainly west of Jones Creek. The surface horizons are very similar to Unit DCT4 but the transported cover is thicker and more complex. A hardpan has developed in the upper 5 m of the profile and overlies either a full or partly truncated lateritic profile. The sequence has three main units, a basal, mottled, puggy clay, overlain by red-brown clays with lenses of lateritic gravel, coarse gravel and an upper horizon of gravely hardpan, 2-5 m thick. The surface is strewn with a coarse, polymictic lag of ferruginous, lithic fragments, maghemite-rich, lateritic gravels, ferruginous saprolite and vein quartz. This sequence is well exposed in the Stellar Pit and described in some detail in Section 6.1.3

6 REGOLITH STRATIGRAPHY, CHARACTER AND PALAEOTOPOGRAPHY

6.1 Stellar

Prior to mining, the Stellar site had a lag-strewn surface on colluvium-alluvium, sloping gently upwards (1:115) to the north (Figure 10A). The thicknesses and basal surfaces of each major regolith unit were contoured (Figures 5A-D). To the south-west, the ground has since been obscured by mine dumps; logging of drill cuttings in this vicinity was not possible. The stratigraphy of the Stellar Pit and details of the palaeochannel stratigraphy and its characteristics are shown in Figures 6-8.

The regolith consists of a cover of colluvial-alluvial and palaeochannel sediments, thickening from 10-22 m from west to east, unconformably overlying Archaean bedrock weathered to 60 m. The following units are recognised:-

i) 0-3 m hardpan developed in coarse gravel;

ii) Red-brown silty clays with lenses of coarse gravel and rounded quartz pebbles (up to 5 mm with low sphericity), having remnant trough bedding;

iii) Laterally persistent, mega-mottled, puggy, smectitic-kaolinitic clays of the palaeochannel;

iv) Residual, lateritically weathered Archaean bedrock.

The lateritic weathering profile appears to be essentially complete but the upper, ferruginous horizon transgresses the unconformity between bedrock and palaeochannel. There is a nodular, vermiform laterite over ultramafic rocks whereas the felsic rocks have an indurated mottled clay with abundant lateritic nodules.

6.1.1 Basement

Distribution

A complete to partly truncated lateritic profile is buried beneath the colluvial and palaeochannel sediments. There are two distinct relationships:- (1) Nodular duricrust forms the principal substrate to the 10 m thick colluvium-alluvium (Figures 6, 9A). These duricrusts are sporadically developed in the pit, to the north-east and to the north-west (Figure 10A). A mottled zone underlies the nodular duricrust and is transitional between saprolite and laterite. A zone of ferruginous saprolite is preferentially developed on ultramafic rocks. (2) The colluvium-alluvium is separated from felsic saprolite by intercalated palaeochannel sediment in the south-east of the pit and extends further to the south-east (Figures 5-9). The base of oxidation is variable but tends to be very deep (generally >60 metres).

Quartz-tourmaline veins in the basement have weathered *in situ* to coarse, rounded cobbles that trace the original projection of the veins well into the laterite horizon. However, similar cobbles are widely dispersed in the upper parts of this horizon, suggesting minor lateral transport, possibly by mass flow. The 'boulder bed' that hosted the supergene mineralisation, first mined at Stellar, may have developed by such mass flow, rather than representing a high energy fluvial deposit. However this material had been mined prior to the commencement of the research.

Stratigraphy and composition

In pit exposures, the laterite forms a semi-continuous horizon from 1.5-2.0 m thick. It merges downwards with a mottled zone, clay zone and saprolite which, in turn, passes into felsic or ultramafic bedrock.

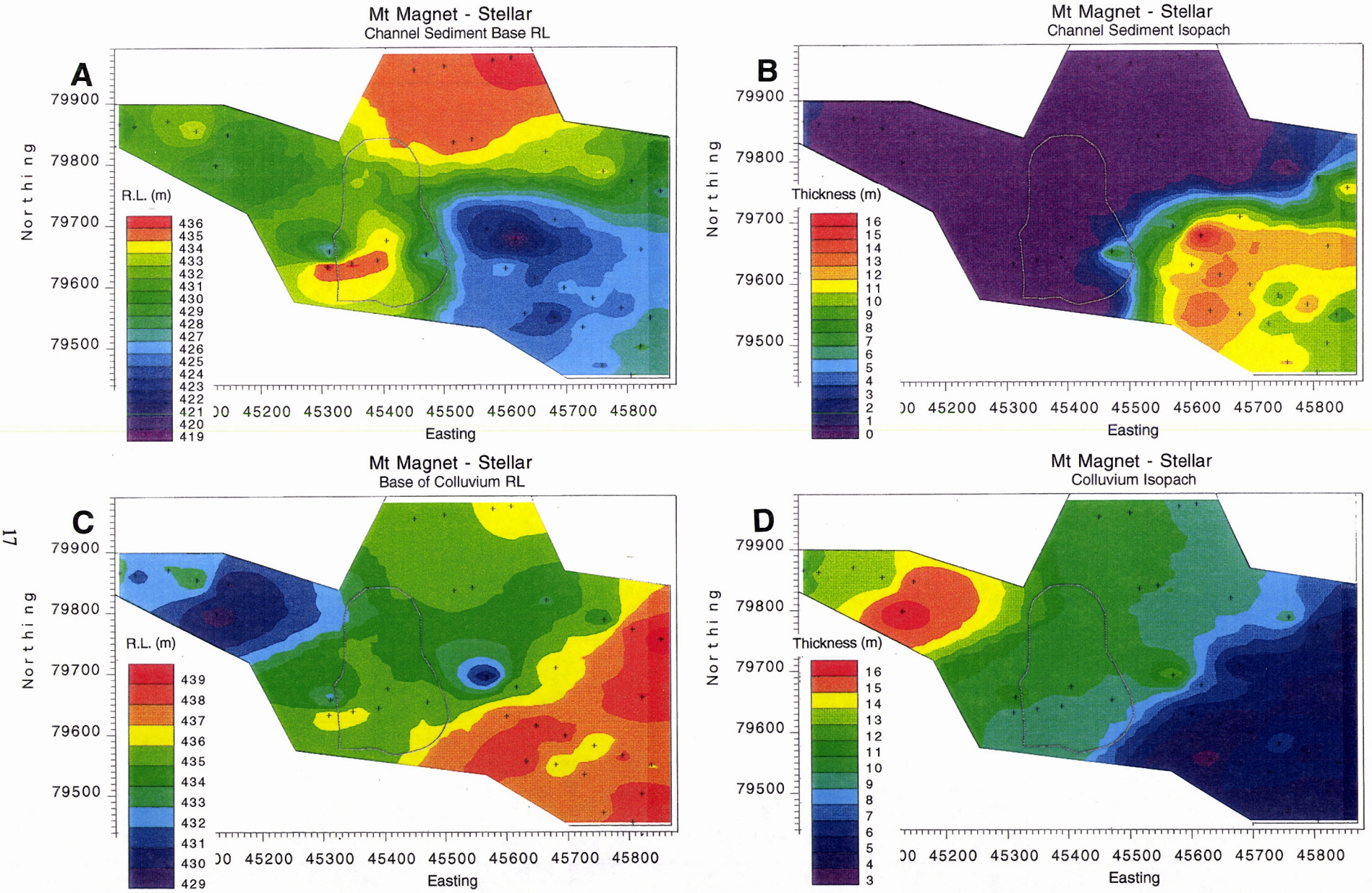

Figure 5. Isopachs and contours of base of palaeochannel sediments (A,B) and of colluvial-alluvial sediments (C,D) at Stellar.

The laterite is nodular to pisolitic and is either weakly-indurated or more strongly cemented as a nodular duricrust. It consists of yellowish brown to reddish brown, goethite-rich nodules, set in a pale to yellowish brown, sandy clay matrix (Figures 11E, F). The nodular duricrust is dominated by goethite and kaolinite, with variable amounts of quartz, hematite, smectite and maghemite. The nodules (5-10 mm) are generally subrounded to irregular and are separated from the porous, kaolinite- and smectite-rich matrix by yellowish-brown cutans up to 0.5 mm thick. Between the nodules, a network of pale kaolinite and quartz patches occur. These have resulted from removal of Fe oxides from the matrix. Irregular to ellipsoidal voids also occur in the matrix, some of which have an earthy infill of kaolinite and quartz. There are no systematic differences in mineralogy between laterites over felsic and ultramafic rocks (Table 1).

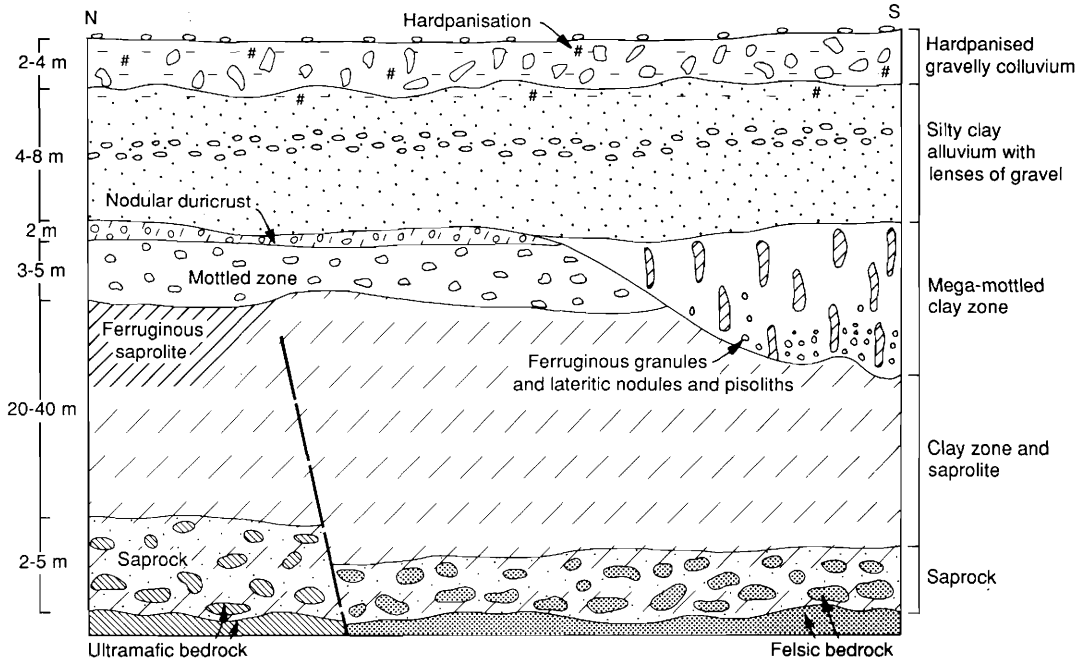

Figure 6. Regolith stratigraphy, Stellar Pit.

In polished section, the matrix of the nodular duricrust and mottled zone from both felsic and ultramafic profiles have abundant, angular grains of detrital quartz (Figures 12A, B). The quartz grains vary widely from 20-200 μm, with a predominance at 50-100 μm. Many quartz grains show corrosion, solution, partial replacement and impregnation by hematite and goethite (Figure 12C). Cores and cutans of some nodules contain quartz but others are quartz free. The iron oxides are dominantly, or a mixture of, goethite and hematite. Some cutans have abundant detrital quartz and retain the fabric of the matrix (Figure 12C).

The geochemical data for felsic and ultramafic profiles are shown in Figure 13 and the compositions of laterite samples developed over the two lithologies are compared in Table 1. The compositions of the lower, weathered layers (upwards to mottled zone) are related to the compositions of their underlying parent rocks (Figure 13). The geochemical characteristics of the parent rock (e.g., Cr, Fe) diminishes from the bottom to the top of the profile but remains evident in the saprolite and mottled clay zones.

However, in the lateritic duricrust, Al, Si, Fe, Mg, Zr, Cr and Ni contents are very similar over both felsic and ultramafic rocks (Table 1) and suggest that the laterite has developed in transported material.

TABLE 1
CHEMICAL COMPOSITION AND MINERALOGY OF FERRUGINOUS MATERIALS -STELLAR

Sample	Type	Bedrock	SiO2	Al2O3	Fe2O3	CaO	MgO	K2O	TiO2	Zr	Cr	Ni	Mn	As	Sb	Au	Mineralogy in
			%	%	%	%	%	%	%	ppm	ppm	ppm	ppm	ppm	ppm	ppb	order of abundance
09-2000	ND	Ultramafic	20.06	16.15	46.34	0.06	0.14	0.03	0.35	80	11606	428	0.031	23	4.9	1300	Gt, K, Hm, Qtz, Sm
09-2001	ND	Ultramafic	17.20	10.38	56.17	0.08	0.24	0.02	0.26	73	8446	326	0.015	194	5.0	870	Gt, K, Qtz, Sm
09-2002	ND	Ultramafic	24.20	14.86	45.48	0.08	0.21	0.04	0.45	120	7940	342	0.018	127	4.2	1490	Gt, K, Qtz, Sm
09-2018	ND	Ultramafic	10.30	20.82	55.71	0.05	0.14	0.02	0.44	140	19018	643	0.024	31	5.8	349	Hm, Gt, K, Mgh, Sm, Qtz
09-2004	ND	Felsic	16.09	14.66	54.14	0.11	0.42	0.05	0.44	140	16391	327	0.021	26	6.3	1510	Hm, Mgh, Gt, K, Qtz, Sm
09-2005	ND	Felsic	25.21	18.29	41.92	0.08	0.23	0.15	0.35	243	7445	186	0.009	26	5.4	403	Gt, K, Qtz, Sm, Hm
09-2019	ND	Felsic	32.31	25.51	25.86	0.10	0.28	0.03	0.64	159	5767	666	0.005	14	2.8	4760	Gt, K, Qtz, Sm
09-2006	FeG	Palaeochannel	12.30	14.99	60.36	0.09	0.29	0.03	0.47	164	19832	405	0.058	42	7.5	25	Hm, Mgh, Gt, K, Qtz
09-2007	FeG	Palaeochannel	10.63	10.53	66.12	0.13	0.31	0.01	0.45	161	18465	301	0.077	46	9.1	<5	Hm, Mgh, Gt, K, Qtz
09-2008	FeG	Palaeochannel	11.41	10.13	65.95	0.12	0.25	0.01	0.44	158	18909	316	0.073	48	10.0	<5	Hm, Mgh, Gt, K, Qtz
09-2009	FeG	Palaeochannel	11.40	12.84	62.08	0.13	0.21	0.02	0.46	157	18792	347	0.050	43	8.2	12	Hm, Mgh, Gt, K, Qtz
09-2010	FeG	Palaeochannel	11.47	12.95	62.08	0.13	0.23	0.02	0.48	154	18822	350	0.051	40	7.6	<5	Hm, Mgh, Gt, K, Qtz
09-2011	FeG	Palaeochannel	12.09	12.47	62.88	0.12	0.20	0.02	0.45	145	17737	317	0.050	52	10.1	16	Hm, Mgh, Gt, K, Qtz
09-2012	FeG	Palaeochannel	13.58	7.38	65.91	0.10	0.30	0.01	1.00	101	4907	277	0.018	23	3.6	<5	Hm, Mgh, Gt, K, Qtz
09-2013	FeG	Palaeochannel	10.44	5.73	73.19	0.12	0.28	0.01	0.96	94	7219	201	0.029	23	4.8	26	Hm, Mgh, Gt, K, Qtz

Analyses by XRF and INAA

ND = Nodular Duricrust
FeG = Ferruginous Granules (2-4 mm)
Gt = Goethite
Hm = Hematite
Mgh = Maghemite
K = Kaolinite
Sm = Smectite
Qtz = Quartz

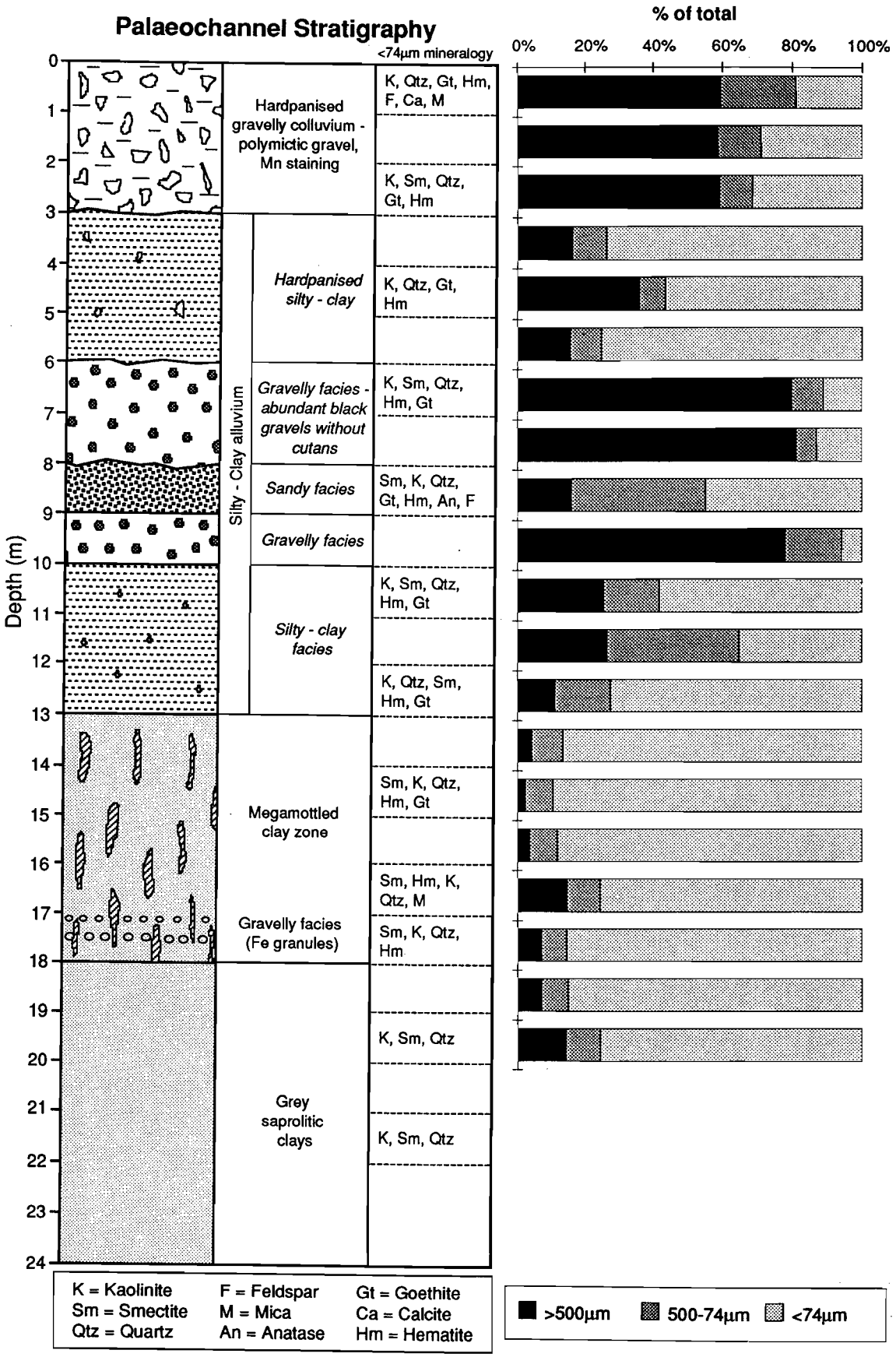

Figure 7. Palaeochannel stratigraphy, mineralogy, distribution of size fractions and characteristics of regolith units, Stellar Pit.

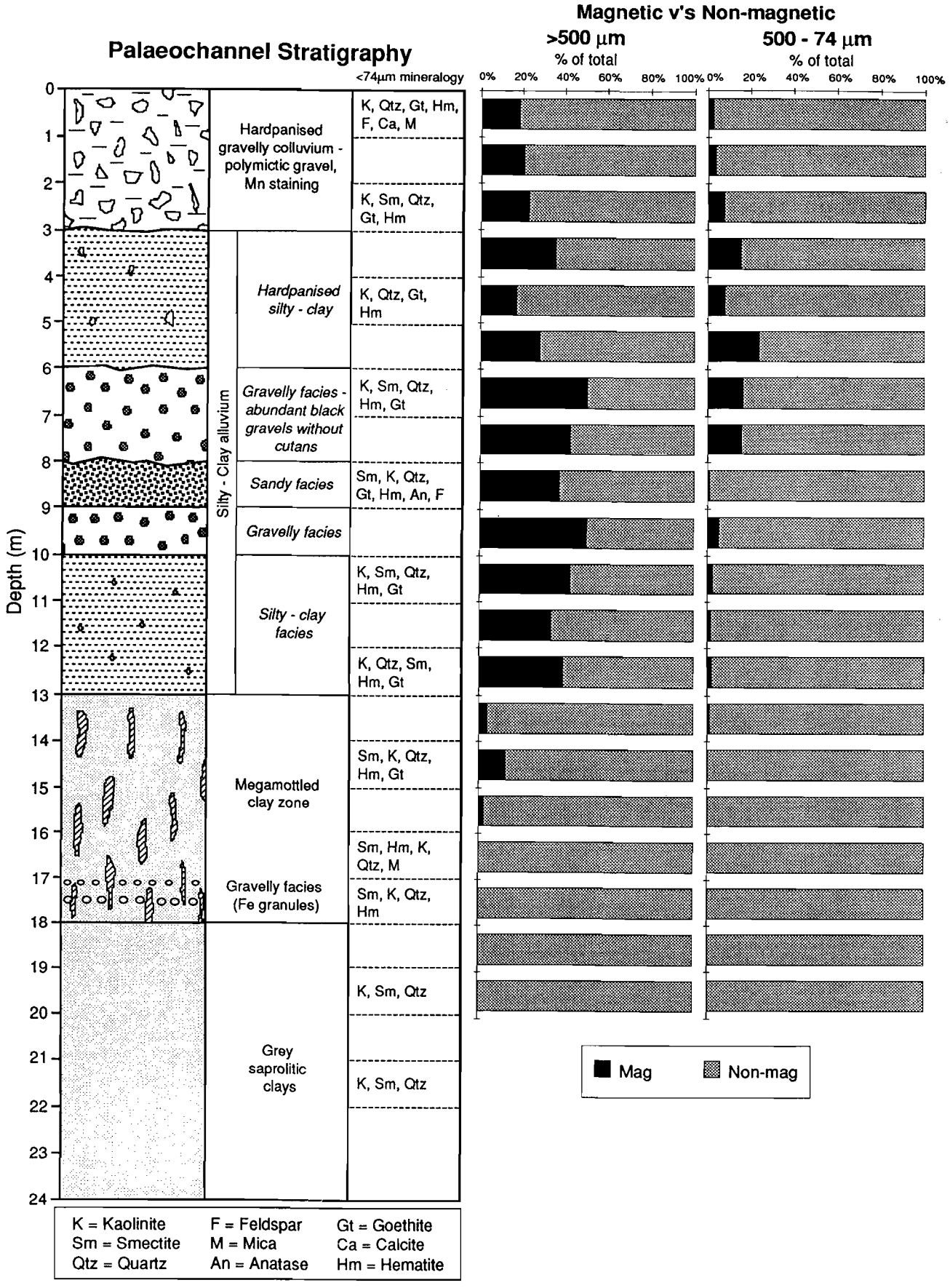

Figure 8. Palaeochannel stratigraphy, distribution of magnetic and non-magnetic components in the >500 µm and 500-74 µm fractions and characteristics of regolith units, Stellar Pit.

Figure 9. Vertical profiles showing regolith stratigraphy of depositional regime.

A. Red-brown silty clay colluvium-alluvium (Ca) overlying poorly indurated, nodular duricrust (Dc). Stellar Pit. Hammer as scale.

B. Mega-mottled clay zone (Cz) (see Figure 9C), developed in palaeochannel sediments, overlain by red-brown, silty clay-rich colluvium-alluvium (Ca). Stellar Pit. Hammer as scale.

C. Delail of vertically elongated, red-brown and yellow, hematitic mega-mottles (Mm), set in creamy-grey smectitic clays (Sc). Stellar Pit. Hammer as scale.

D. Hardpanised red-brown colluvium-alluvium (Ca) overlying saprolite (Sp). Quasar Pit. Hammer as scale.

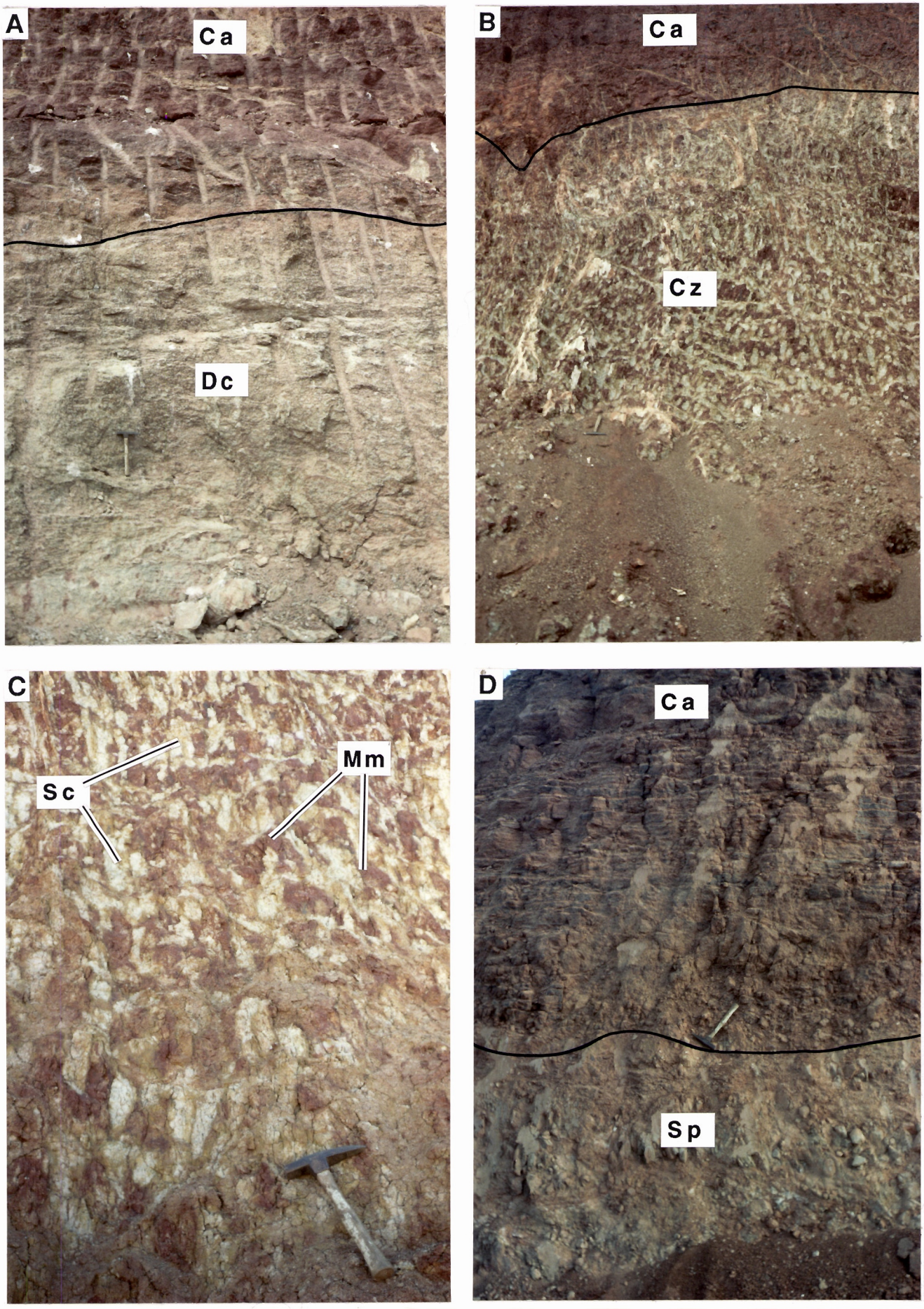

Figure 9. Vertical profiles showing regolith stratigraphy of depositional regimes at Stellar and Quasar.

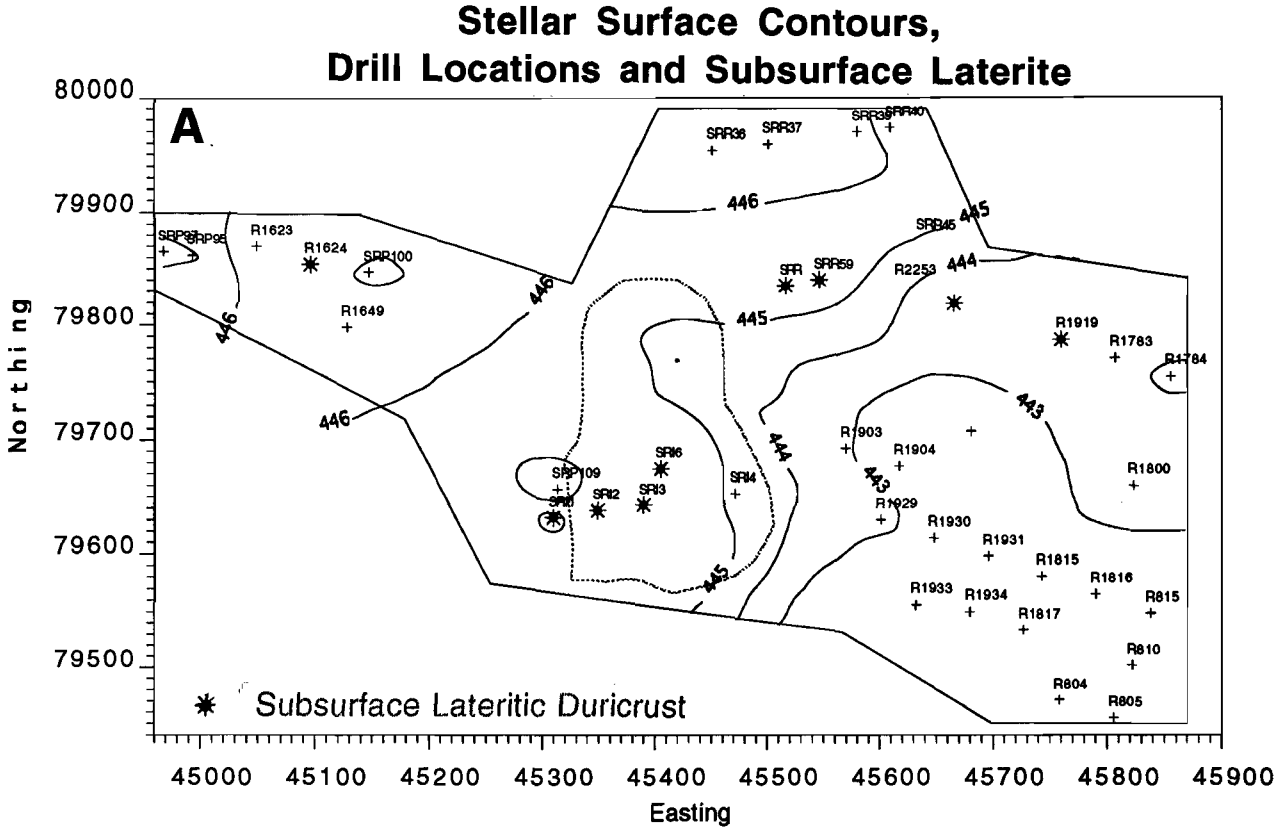

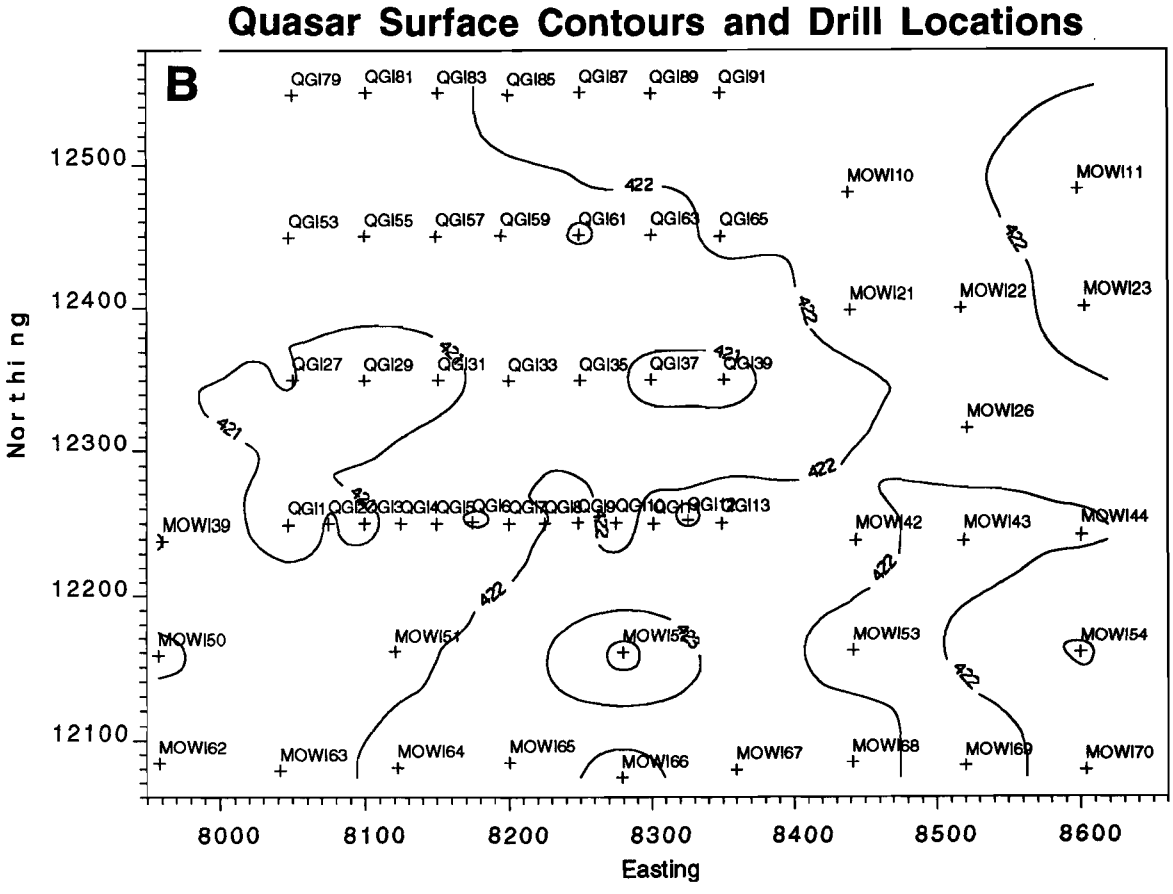

Figure 10. Surface contours and drillhole locations for Stellar (A) and Quasar (B).

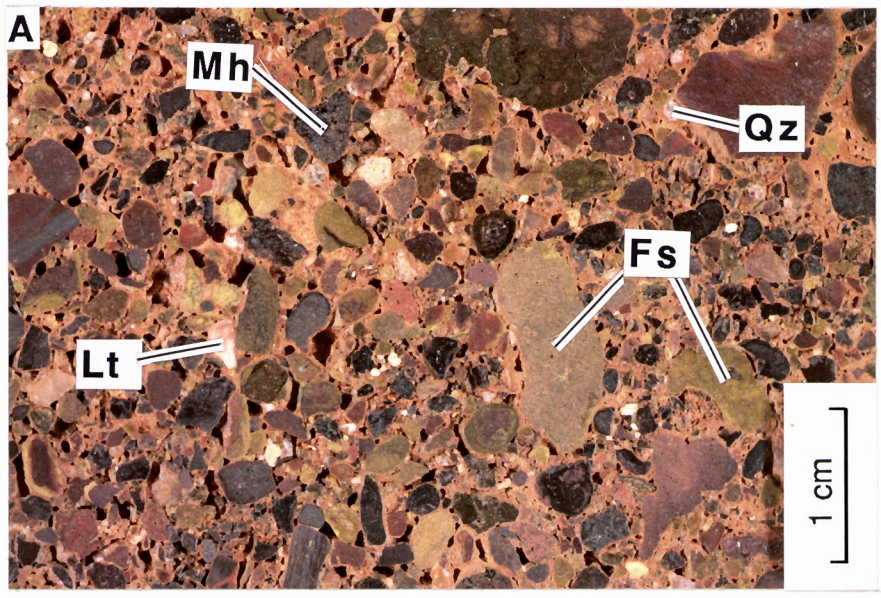

Figure 11. Close-up photographs of regolith materials from Stellar

Colluvium-alluvium

A. Clast-supported gravelly colluvium-alluvium showing maghemite-rich lateritic nodules (Mh), ferruginous saprolite fragments (Fs), lithic fragments (Lt) and granules of quartz (Qz) in a silty-sandy matrix. Specimen QHC3.

B. Matrix-supported, silty-clay colluvium-alluvium with a few maghemite-rich clasts (Mh) and lithic fragments (Lt) Specimen SGC1.

Ferruginous materials in palaeochannel

C. Resin-impregnated grain mount of granules from mega-mottled clay horizon, containing ferruginous granules (Fg), quartz clasts (Qz) and lateritic pisoliths with cutans (Lt). Specimen ST6A. Co-ordinates 79885 mN, 45421 mE.

D. Subrounded to subangular nodules and pisoliths (Np) in a partly Fe-stained, smectite-rich matrix (Fs). Specimen ST6A. Co-ordinates 79885 mN, 45421 mE.

Nodular duricrust

E. Nodular duricrust over felsic bedrock containing goethite-rich lateritic nodules (Gt) and lithic fragments (Lt) in a kaolinite- and smectite-rich matrix (Ks). Banding in matrix due to leaching of Fe. Specimen 09-2004. Co-ordinates 78889 mN, 45372 mE.

F. Nodular duricrust over ultramafic bedrock containing goethite-rich nodules (Gt) and kaolinite-rich void infillings (Kv) in a goethite- and kaolinite-rich matrix (Gk). Specimen 09-2002. Co-ordinates 79943 mN, 45297 mE.

Figure 12. Photomicrographs of polised sections of duricrust from Stellar.

A. Goethite- and hematite-rich nodule (Gh) in a quartz-rich matrix (Qm) developed over a felsic parent rock. The nodule has a continuous, lead-grey cutan (Cn) of goethite Specimen 09-2004. Normally reflected light.

B. Hematite- and goethite-rich nodule (Gh) is set in a quartz-rich matrix (Qm), developed over an ultramafic parent rock. Specimen 09-2002. Normally reflected light.

C. Cutan with abundant detrital quartz (Qn) and a quartz grain (Qz) are set in a goethite-rich nodule (Gn), developed over an ultramafic parent rock. Specimen 09-2018. Normally reflected light.

D. Gold (Au) as wire-shaped and platy particles and subhedral to anhedral crystals are included in a goethite and hematite-rich nodule (Hm) from nodular duricrust Specimen 09-2018. Normally reflected light.

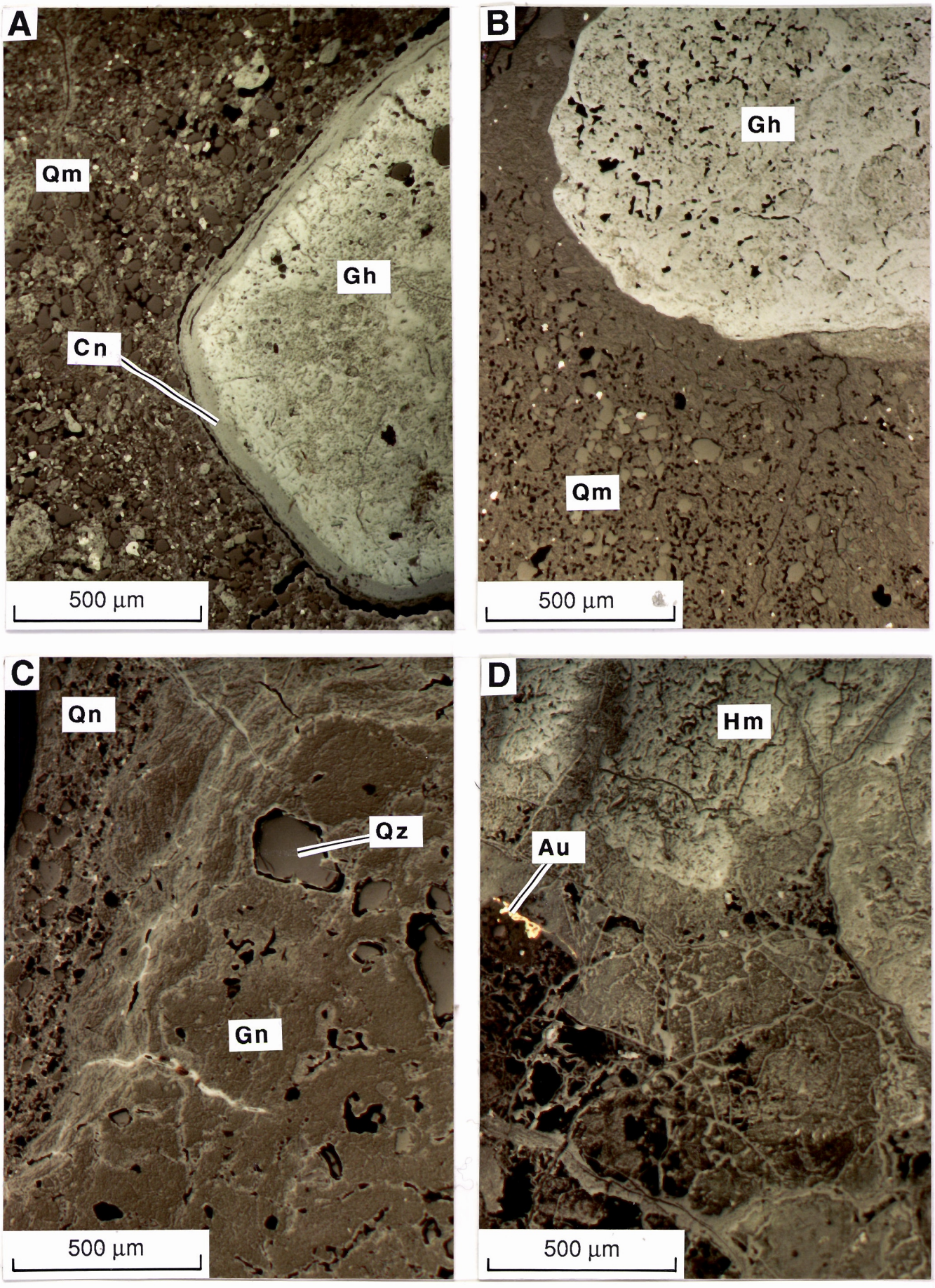

Figure 12. Photomicrographs of polised sections of duricrust from Stellar.

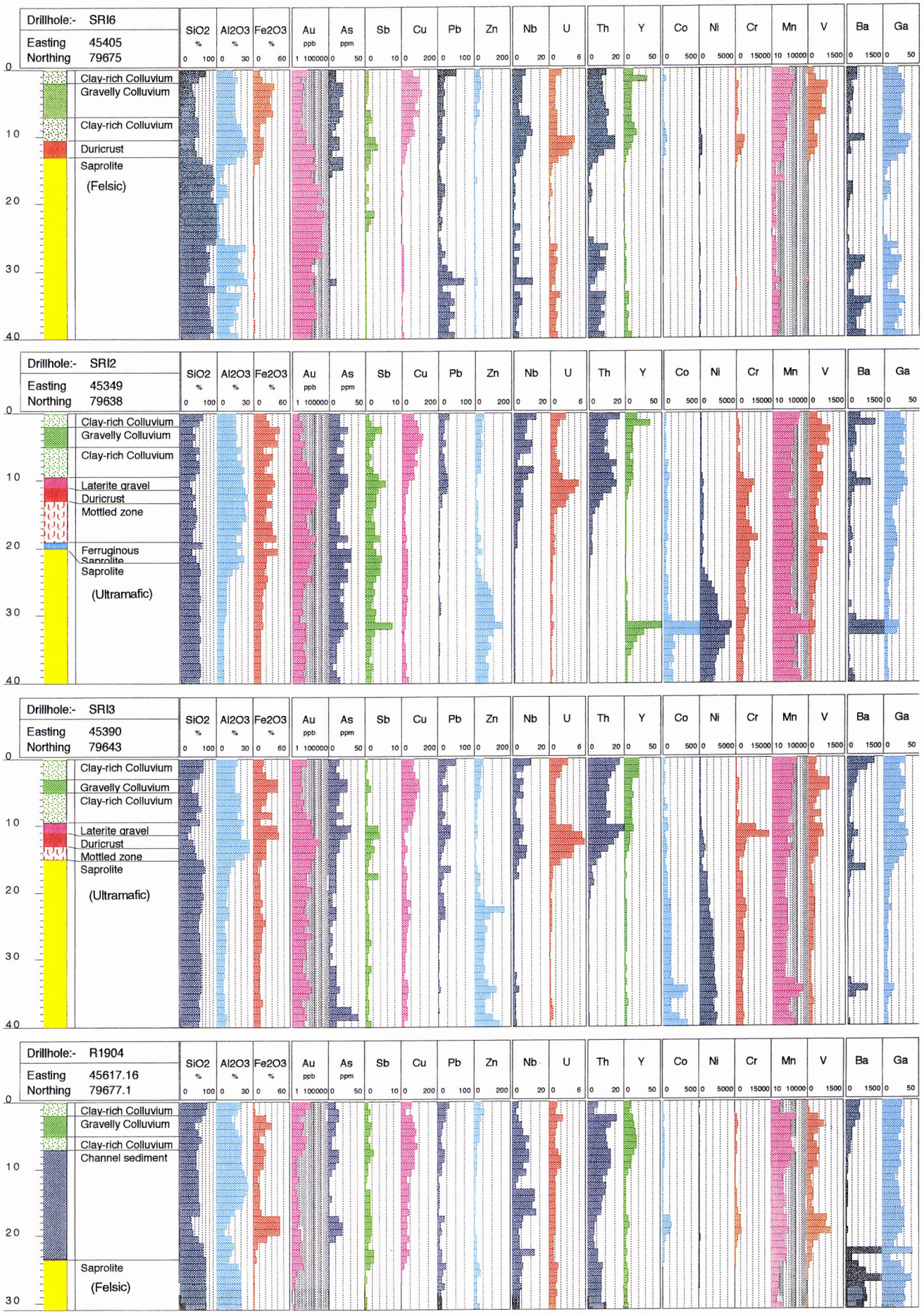

Figure 13. Vertical distribution of elements in felsic and ultramafic profiles at Stellar.

There are significant concentrations of Au (349-1490 ppb) and As (14-194 ppm) in the lateritic duricrust over felsic and ultramafic rocks (Table 1). Free Au occurs in the nodules as irregular, subhedral to anhedral crystals and as delicate wire forms (20-100 μm) on the surfaces of goethite or hematite (Figure 12D). In detail, the Au crystals show dissolution and surface pitting. The close association of Au and Fe-oxides, and the morphology of the Au, indicates that the Au is dominantly secondary.

6.1.2 Palaeochannel sediment

Distribution

The sediments of the palaeochannel (Figure 6) are well exposed in the south-east wall of the pit, are unconformable on the basement and extend to the east and south east (Figure 5B), reaching a maximum thickness around drillhole R1904 (Figures 5B and 13) of 18 m. The residual regolith surface, onto which the palaeochannel sediments were deposited, probably had a palaeohigh to the north and a localised palaeohigh in, what is now, the south-west wall of the pit, although some modification of the landscape probably occurred prior to colluvium-alluvium deposition. The area east and south-east of the pit had been eroded into a curved channel (Figure 14A), possibly with an entry point to the east and an exit to the south. The north and north-west wall of the channel was steep (1:10) but the south-east part sloped quite gently upward (1:75) to the south-east. The upper part of the residual regolith, along the steep flank of the channel (Figure 10A), is formed by duricrust.

Stratigraphy and composition

The sediments of the palaeochannel, which are overlain unconformably by colluvial-alluvial Quaternary sediments, consist of a grey, plastic clay and minor sandy clay (smectite and kaolinite) (Figures 9B, C). Hematitic brown and yellow mottles occur as vertically elongate aggregates up to 400 mm long (Figure 9C). Creamy, grey clays become more prominent with increasing depth and contain elongate, columnar cracking structures which expose roots, commonly sheathed in Fe-rich accumulations. This mega-mottled horizon is typical of palaeochannel environments in the Yilgarn (Anand *et al.*, 1993b; Singer, 1979; Kern and Commander, 1994).

An irregular horizon of sepiolite masses occurs towards the top of the palaeochannel. Sepiolite has been reported in both marine and lacustrine environments and is abundant in some valley calcretes in the Yilgarn (Butt *et al.*, 1977). It is generally associated with aquatic, alkaline conditions, with high activities of Si and Mg.

Two types of ferruginous materials occur towards the base of this unit; small, black granules (2-5 mm) and lateritic nodules and pisoliths (4-10 mm; Figures 11C, D). The mottles contain abundant, angular to well-rounded, black, ferruginous granules, lateritic nodules and pisoliths, ferruginised lithic fragments and quartz grains. Lateritic nodules and pisoliths are also scattered throughout the clay. The cores of the granules have an earthy to silvery, metallic lustre and a few have a thin, earthy cutan; some are magnetic, some are non-magnetic. The granules, nodules and pisoliths largely consist of hematite and maghemite, with small amounts of goethite, kaolinite and quartz. At present, their origin is unclear; it appears that, although many have been transported, some have developed *in situ* in the clays. The compositions of ferruginous granules separated from the mega-mottled clay zone are given in Table 1. They consist largely of hematite and maghemite, with small amounts of goethite, kaolinite and quartz. They are comprised mainly of Fe_2O_3 (>62%), SiO_2 (10-12%) and Al_2O_3 (5-15%). These ferruginous granules are characterised by high concentrations of Cr, Ni and low concentrations of Au and As. This contrasts with the lateritic duricrust, which has greater concentrations of Au.

6.1.3 Colluvium-alluvium

Distribution

The thickness of colluvium-alluvium increases to the north-west (Figure 5D). The surface on which it was deposited was stepped and sloped downwards to the north-west. Prior to colluvium deposition, there was a palaeohigh to the east and south-east of the site of Stellar Pit, a steep gradient (1:35) close to the south-east pit wall, a relatively gentle slope (1:120) throughout the pit area and a further steep gradient (1:20) to the north-west, leading to a low point around drillhole R1649. This palaeotopography suggests reversal of gradients since the beginning of deposition of the palaeochannel sediments; it implies that palaeochannel sediments may have been more widespread, overlying the residual regolith throughout, and to the north-west of the Stellar Pit, but have since been eroded. Mechanical dispersion of any palaeosol developed on the residual regolith at this time would have been generally to the north-west.

Stratigraphy and composition

The colluvium-alluvium is composed of two sedimentary units: a lower, red-brown, silty clay with coarse, gravelly lenses, rounded quartz pebbles and remnant trough bedding and an upper hardpan from 0-3 m depth, in the coarse gravel. Each unit consists of several facies (see Figures 7 and 8). The colluvium-alluvium was separated into three size fractions; >500 μm, 74-500 μm and <74 μm. The <74 μm fraction was analysed mineralogically. Results are shown in Figures 7 and 8.

Hardpanised gravelly unit : The upper colluvium-alluvium is an approximately three metre thick, polymictic, gravel-dominated unit, composed of a variety of clasts, including fine- to medium-sized, lateritic nodules and pisoliths (4-15 mm) and fragments of BIF, vein quartz and ferruginous saprolite in a red brown, sandy-silt matrix (Figures 11A, B). The sand is generally poorly sorted and the quartz grains are angular, suggesting a proximal source. The clasts in the gravel are both magnetic and non-magnetic, rounded to angular, unsorted and up to 40 mm in diameter. Their variety indicates diverse origins, including breakdown of lateritic duricrust, saprolite and BIF. The <75 μm fraction largely consists of kaolinite and quartz, with small amounts of goethite, hematite, feldspar, calcite and mica (Figure 7). Red-brown hardpan is strongly developed in this unit and is brittle, dull, porous, laminar and partly silicified. Accumulations of black Mn oxides are characteristic and occur on subhorizontal partings and on vertical fracture-surfaces.

Hardpanised silty-clay unit: This underlies the gravelly unit and is only moderately indurated and weakly hardpanised. Its thickness varies from 4-8 m. In places, where erosion of laterite and mottled zone has occurred, and the clays of the palaeochannel are absent, it lies directly on saprolite. This unit appears conformable with the overlying hardpanised gravelly unit but it lies unconformably on underlying units. The latter relationships are exposed at Stellar, where the hardpanised silty-clay unit overlies buried laterite and extends over, and partly erodes, a mega-mottled clay horizon. There are three facies, with each being laterally continuous across the pit face.

Facies 1 consists of red-brown silty-clay, up to three metres thick, and is dominated by kaolinite and quartz, with small amounts of goethite and hematite (Figure 7). It appears to be derived from erosion of saprolite.

Facies 2 is 1-2 m thick and occurs as lenses of well-rounded, reddish brown to black lateritic gravels (without cutans) and rounded pebbles of vein quartz within the silty-clay facies and represent transported lateritic debris. These lenses are generally thinner than those of the fine-grained, silty-clay, alluvial materials. A sharp boundary separates facies 1 and 2 and is marked by a difference in appearance in the gravels. Magnetic, lateritic gravels of hematite and maghemite dominate the gravel fraction (Figure 8). Beds of lithic fragments are rare. This

material appears to have been derived from erosion of a laterite. The <75 μm fraction largely consists of kaolinite, smectite and quartz with small amounts of hematite and goethite.

Facies 3 comprises sand to sandy clay, up to one metre thick. Its <75 μm fraction consists largely of smectite, kaolinite and quartz with small amounts of goethite and hematite (Figure 7). It appears to have been derived from erosion of saprolite.

6.2 Quasar

Reconstruction of the original surface from drill collar information (Figure 10B) shows that the ground was nearly flat to the west with a very low, arcuate, approximately north-trending ridge in the centre and east. This surface was strewn with polymictic lag. The distribution of drilling was sufficient to give a relatively accurate picture of the palaeotopography.

6.2.1 Basement

The bedrock is overlain by about five metres of hardpanised colluvium-alluvium (Figure 9D). The basement consists of weakly mottled, clay-rich ultramafic saprolite, kaolinitic saprolite and silicified felsic-porphyry. Some weak mottling occurs in the clay-rich, felsic saprolite, where the base of oxidation deepens towards the structural contact. The base of oxidation on the ultramafic rocks is around 35 m; on the felsic rocks, the depth of weathering is variable, from a few metres to >40 m near the shear zone.

6.2.2 Palaeochannel sediment

The palaeochannel sediments were restricted to the south-west and were deposited in an arcuate channel (Figure 14A) eroded into the basement; the flow direction was possibly to the south-west. As at Stellar, the channel has a steep gradient on its northern margin and a lesser gradient to the south. The palaeochannel isopachs (Figure 14B) indicate a general thickness of three metres with local maxima of six metres, hence it is shallower and smaller than the palaeochannel at Stellar. The sediments consist of white, kaolinitic clays with distinct layers of lateritic gravels (with cutans). There are no exposures of palaeochannel sediments in the pit.

6.2.3 Colluvium-alluvium

The basement on which the hardpanised colluvium-alluvium was deposited (Figures 14C and 9D) slopes downwards to the south, suggesting that either the depression in which the palaeochannel sediments were deposited was incompletely filled or this area was partly eroded after deposition of these sediments. The gradients, prior to deposition of the colluvium, were gentle (1:80) and the thickness of the colluvium (Figure 14D) is quite consistent (4-8 m), in contrast to that at Stellar. Mechanical dispersion of any palaeosol developed on the residual regolith, just prior to deposition of the colluvium, would generally have been to the south.

The colluvium-alluvium is composed largely of lateritic nodules and pisoliths, with and without cutans, and fragments of quartz and ferruginous saprolite, in a silty-clay matrix. Fragments of jaspilite, chert and BIF generally occur in the upper two metres of the profile, with lateritic debris dominant at lower levels. The upper part of this transported overburden consists of poorly-sorted gravels with coarse, angular fragments of quartz and lithic material, typical of colluvium. Towards its base, the transported cover becomes matrix dominated, with coarse, poorly sorted, gravelly lenses, consisting of rounded quartz pebbles and lateritic debris, indicating an alluvial environment. Manganese oxide staining is strongly associated with matrix-dominated horizons.

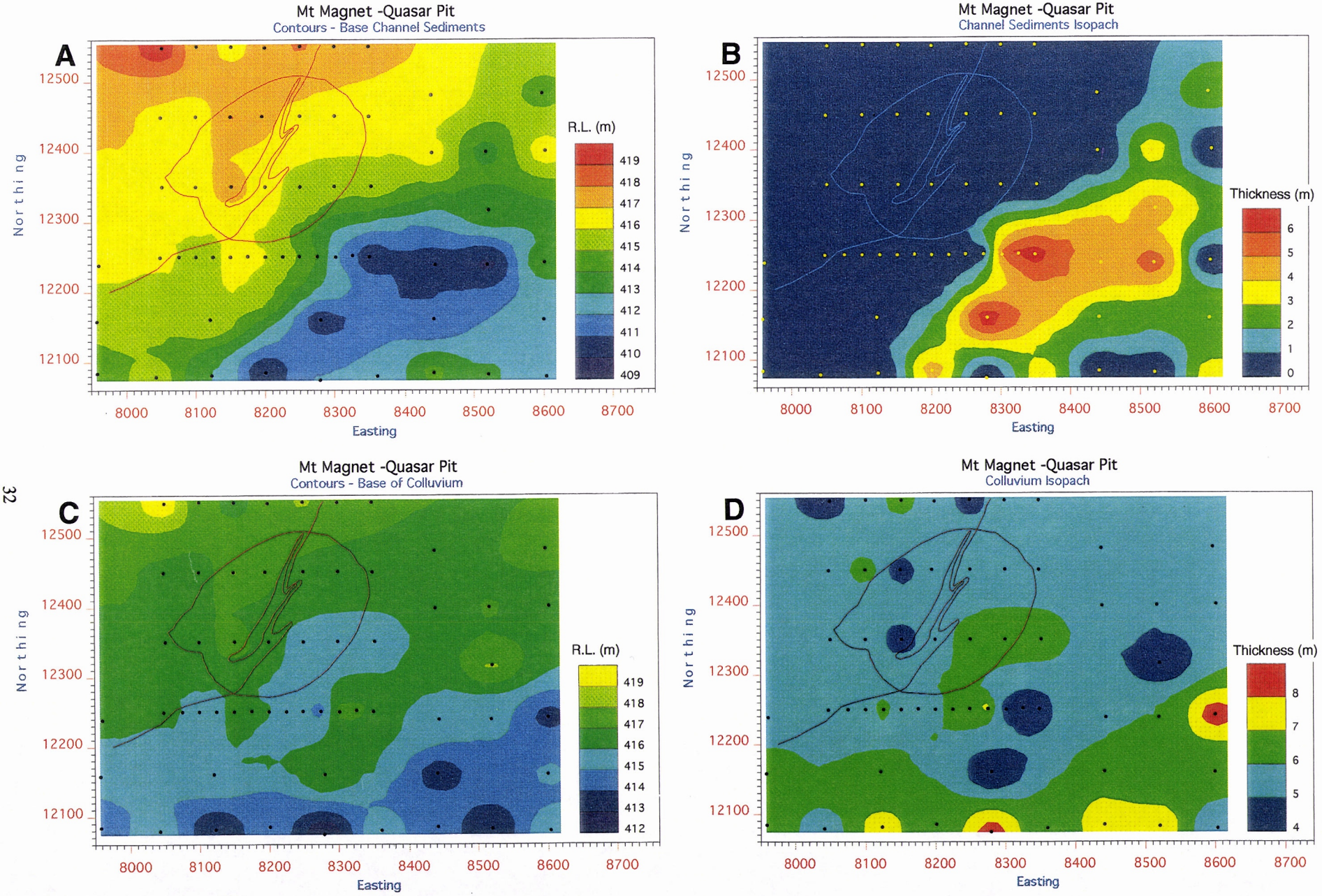

Figure 14. Isopachs and contours of base of palaeochannel sediments (A,B) and of colluvial-alluvial sediments (C,D) at Quasar.

7 GEOCHEMISTRY

7.1 Background and threshold abundances

The complex, multilayer regolith, with at least two types of transported cover over a variably stripped residual regolith, derived from contrasting felsic and mafic-ultramafic rocks, has made reliable determination of background and threshold geochemical abundances particularly complex. Because most of the geochemical sampling was close to mineralisation, estimated threshold abundances can only be considered as local (Rose, Hawkes and Webb, 1981). However, because of the highly mineralised nature of the bedrock, the district to regional scale background would be difficult to establish, even with a widespread array of sample points.

Table 2 gives background and threshold abundances determined by inspection of probability plots and contoured data. The data set for the palaeochannel sediments was regarded as too small for these estimations. It must be emphasised that these estimates were determined for a very limited area. The databases for Quasar and Stellar are tabulated in Appendices Q1 and S1. Frequency distributions are shown in Appendices Q2 and S2. Spearman Rank correlations have been investigated within the untransformed data sets in Appendices Q3 and S3.

TABLE 2
LOCAL BACKGROUNDS AND THRESHOLDS

	Colluvium		Lag		Interface		Top Archaean	
	Back-ground	Thres-hold	Back-ground	Thres-hold	Back-ground	Thres-hold	Back-ground	Thres-hold
As	15	25	35	45	10	20	15	35
Au	50	100	60	200	30	80	50	200
Ba	400	500	60	140	450	630	400	620
Bi	0.5	1.0	0.7	1.3	0.4	0.8	0.5	1.0
Co	30	40	20	25	20	35	10	20
Cr	1300	2200	2000	2250	400	1200	200	800
Cu	80	120	130	150	25	65	25	60
Fe	20	25	30	38	3	5	3	5
Ga	25	30	27	30	20	26	15	19
Mn	500	700	400	700	400	600	200	330
Nb	3	5	2	4	3	4	2	4
Ni	200	320	100	120	200	400	200	600
Pb	10	40	25	45	10	25	15	100
Sb	2	10	2	4	3	7	1	2.5
Th	10	12	14	17	6	7.9	5	7
U	1.4	1.7	2.5	3.0	1.0	1.4	1.0	1.4
V	400	600	900	1100	150	250	100	200
Y	15	20	6	8	6	12	4	8
Zn	45	60	50	80	30	50	20	45

There is a wealth of data from 58 drillholes through the regolith at the Quasar deposit and its surroundings. It is difficult to represent such data in three dimensions in a manner that can be

readily visualised and understood. Accordingly, the data are presented in both selected sections (Appendix Q10) and in plan (Appendices Q6-Q8); for the latter (Section 7.3), distributions of individual elements and element combinations are shown for several possible sample media to compare their usefulness in exploration.

The amount of geochemical data from Stellar is much less, being restricted to seven drillholes, and is plotted as bar charts in Figure 13. Although this is insufficient for a satisfactory dispersion study, the greater variety of regolith types made it particularly useful for a study of regolith type discrimination (Section 7.4.1).

7.2 Dispersion in section

7.2.1 Stellar

Colluvium-alluvium

There is a generally high Au background in the colluvium, particularly apparent in background drillhole R1904, where the Au content of the colluvium greatly exceeds that of the palaeochannel and the saprolite (Figure 13). This presumably reflects imported detritus from the extensively mineralised areas of the region rather than proximity to Stellar. The high background in the colluvium represents one of the major problems facing exploration in the Boogardie Synform. The colluvium tends to be comparatively enriched in Cu, Zn, Nb, Y and V relative to other regolith units. The upper parts of the colluvium tend to be Pb and Ba-rich (Figure 13).

Palaeochannel sediments

The palaeochannel sediments are particularly poor in Ni, Ba and Au. There is an increase from 10-15% to >40% Fe_2O_3 between 17 and 21 m in the palaeochannel sediment of R1904, with sympathetic increases in As, Pb, Y, Co, Cr and V (Figure 13), possibly reflecting the presence of ferruginous detritus or authigenic materials.

Lateritic gravel, duricrust, ferruginous saprolite and mottled zone

The lateritic gravel on the duricrust, the duricrust, ferruginous saprolite and mottled zone, where they occur, are marked by concentrations of U and Cr and weakly in Ba. Nickel is depleted relative to the saprolites below. They are relatively rich in As and Sb (~15-35 ppm and ~2-8 ppm respectively) but these contents seem related more to the abundance of Fe than to mineralisation. They are rich in Au (~1000 ppb) within the pit area and formed a supergene deposit here. There is no information from Stellar to estimate background Au abundances in these regolith materials.

Clay saprolite and saprolite

Distal from mineralisation (R1903, R1904) Au is generally around 10-50 ppb; proximal to mineralisation (SRI1, SRI2, SRI4) it is at abundances of 10-2000 ppb and within mineralisation (SRI3, SRI6), Au in the saprolite is in the range 20-20000 ppb. Although the As and Sb abundances in the saprolite of R1903 and R1904 are low compared to others, it is thought these reflect abundances in felsic rocks compared to mafic-ultramafic saprolites, where the As and Sb abundances are greater but seem unrelated to mineralisation. Thorium, U and Y are depleted in the lower residual regolith, only where upper regolith materials are present. Where these upper regolith materials have been eroded and replaced by palaeochannel sediments, these elements are more evenly distributed in the lower regolith. Zinc is less depleted in the lower regolith than in the duricrust and related materials. Elevated Fe, Cr, Ni and Co in the saprolite are indicative of mafic-ultramafic bedrocks.

Interface

At Stellar, there is a suggestion that Au concentrations at the base of the colluvium-alluvium are significantly greater (100-170 ppb) than in its bulk (20-50 ppb) in drillholes over (SRI3, SRI6) or proximal (SRI2) to mineralisation. Au accumulations at this unconformity in drillholes distal

to mineralisation (SRI1, SRI4) and in background localities (R1903, R1904) are in the range of 20-50 ppb. This provides some support, from Stellar, of the efficacy of interface sampling, established below (Section 7.3.1) at Quasar.

7.2.2 Quasar

Three sections have been examined in detail. The data plots are shown in Appendix Q10:-

i) 12100 mN, comprising 9 holes drilled between 12070 and 12100 mN, projected onto the same section. This passes well south of the main mineralisation.

ii) 12250 mN, comprising 13 holes on 12250 mN and four on 12240 mN, projected onto the same section. This passes just south of the main mineralisation.

iii) 12350 mN, comprising 7 holes on 12350 mN and three on 12400 mN, projected onto the same section. This passes through the mineralisation.

Cutter values were selected from cumulative frequency plots of the whole data set, to identify separate populations and subdivide large populations. Element distributions are interpreted relative to the three principal units that comprise the regolith in section:-

i) Colluvium, 4-5 m thick, hardpanized in the top 2-3 metres and becoming more clay-rich with depth.

ii) Palaeochannel sediments, dominantly mottled clays, 5-8 m thick, occurring in the east of the sections. The palaeochannel appears to be intermittent for over 400 m on 12100 mN, about 300 m wide on 12250 mN and is reduced to about 100 m on 12350 mN. On 12250 mN, the sediments appear to form a palaeohigh relative to the base of the overlying colluvium, suggesting that there was an erosional event prior to colluvium deposition.

iii) Saprolite, clay-rich near the unconformity in deeper profiles, becoming harder and merging to saprock at the base.

The unconformity between the sediments (colluvium and palaeochannel clays) and the saprolite is represented by a 1-2 m thick interface of mixed sample materials. The main lithologies of the Archaean, mafic-ultramafic and felsic, can be distinguished in the saprolite by a range of elements; this geochemical contrast is not evident in the raw data in the sedimentary overburden. In comparison, the overburden is laterally relatively uniform, although having some vertical stratification. It is not possible to determine from this data set whether the Au content of colluvium (50-90 ppb) is a regional feature, or whether it indicates the presence of concealed mineralization and therefore provides a useful sample medium. Apart from Au, only Bi seems to indicate mineralization in saprolite on the section studied. Although there is a trace of Bi present in the colluvium close to mineralization, the distribution is spotty and may be an artefact (e.g., *analytical*, because abundances are close to detection limit; or *contamination,* during drilling, by material from the previous drillhole). Arsenic and Sb abundances are mostly low, although anomalous concentrations of both elements (10-50 ppm Sb; 40-140 ppm As) are present in colluvial and palaeochannel sediments on the east of the sections, suggesting a provenance from the east or south east. Such a provenance, which is also indicated by the distributions of Ni and Cr, is illustrated by the mean abundances in colluvium (Appendix Q6). Neither Pb nor Zn distributions seem to reflect the presence of mineralization, either in the saprolite or in the transported overburden.

The *gold* content (Appendix Q10/2) exceeds 50 ppb in all colluvial samples, with some >90 ppb (maxima to 120 ppb), particularly where the colluvium directly overlies saprolite. In comparison,

palaeochannel clays contain <12.5 ppb Au. Saprolite commonly contains <12.5 ppb Au, but concentrations rise towards the unconformity. Many of the higher Au contents in the section seem to occur close to the interface, suggesting that this has potential as a preferred sample medium. However, where palaeochannel sediments are present, the colluvium/palaeochannel sediment interface has higher Au contents than the palaeochannel sediment/saprolite interface. Either there was a low Au abundance in the basement in this zone or erosion, prior to palaeochannel deposition, removed any palaeosol developed on the weathered Archaean and any contained anomaly. Maximum Au concentrations of 200-500 ppb occur in upper saprolite in QGI7 and QGI8 (12250 mN) and QGI33 (12350 mN), and represent the upper weathered part of the mineralized shear.

Arsenic contents (Appendix Q10/1) are generally very low, being less than 5 ppm on most saprolite, and only 12-15 ppm in drillhole QGI27 and the mineralized intersection in QGI33. Concentrations are uniformly greater in the colluvium-alluvium (12-15 ppm, increasing to 20 ppm, locally >50 ppm in the east); palaeochannel sediments contain >20 ppm As. The As distribution broadly follows that of Fe.

Bismuth contents (Appendix Q10/4) are generally <1 ppm, but trace amounts (>4 ppm) occur in QGI27, QGI29 QGI33, on 12350 mN, and at the base of MOWI43, on 12250 mN. Bismuth occurs sporadically at 1-2 ppm in colluvium-alluvium above saprolite in the vicinity of mineralisation (QGI27, QGI29 and QGI33 as above). This may reflect the presence of Bi in saprolite, or indicate contamination. No anomalous Bi was detected in any sample on section 12100 mN, 200 m south of the orebody.

Antimony concentrations (Appendix Q10/15) are generally low (<3 ppm) in saprolite and colluvium-alluvium. However, there are some much higher concentrations (10-52 ppm) in the palaeochannel clays and colluvial sediments above and adjacent to the clays, principally on 12250 mN and 12100 mN. This suggests provenance from the east or south-east.

There is a very spotty *lead* distribution (Appendix Q10/14), with no significant difference between saprolite and overburden (abundances of 5-25 ppm Pb, with scattered greater concentrations of 40-50 ppm). The lowest abundances occur in saprolite in the western part of section 12350 mN. There is no difference between mineralised and unmineralised units; the occurrence of increased abundances in saprolite seems as great in the latter as in the former.

There are uniform abundances of 35-70 ppm *zinc* in the colluvium-alluvium (Appendix Q10/20), with a few samples containing up to 100 ppm in the west of the sections. The palaeochannel sediments, however, contain <35 ppm Zn. Saprolites on mafic-ultramafic rocks generally contain 70-100 ppm Zn (maximum 120 ppm), in the lower part of the profile, whereas felsic rocks contain < 70 ppm throughout.

Iron, chromium, copper, cobalt, manganese, nickel and vanadium (Appendix Q10/6-9, /11, /13, /18) have generally similar distributions. Abundances in the colluvium-alluvium are broadly uniform, with all but Mn tending to increase with depth; concentrations in the palaeochannel sediments are rather less. The surface enrichment of Mn is associated with hardpan, within which Mn oxides occur as thin coatings on partings. Saprolites, derived from mafic-ultramafic rocks (QGI27, QGI29, QGI31, QGI33, on 12350 mN; QGI1, on 12250 mN; MOWI70, on 12100 mN) have similar abundances of these elements as the overlying colluvium-alluvium, although there is some leaching for three to four metres below the unconformity. Saprolites on felsic rocks tend to have uniformly low abundances in these transition elements, consequently each of these elements effectively discriminates between these broad lithologies.

Calcium data (Appendix Q10/5) are unreliable at low abundance levels but may be acceptable above about 1%. Low Ca contents are found in the colluvium-alluvium (<1%, mostly <0.3%) and in the upper saprolite (<0.1%), especially on felsic rocks. Higher concentrations (>2%) are present in a sub-horizontal zone close to the interface in colluvium-alluvium and saprolite and within the palaeochannel sediments, possibly reflecting precipitation of secondary carbonates. Dolomite was noted in some palaeochannel sediments. Similarly high Ca contents in the mid- to lower saprolite, however, probably reflect the presence of relict primary minerals.

The colluvium-alluvium contains 350-550 ppm *barium* (Appendix Q10/3), with higher concentrations in the top 1-2 m. The palaeochannel sediments have rather lower (<350 ppm) Ba contents. Abundances in saprolite are generally higher (>550 ppm) than in the overburden, although there is some leaching apparent in clay saprolite in some profiles on mafic-ultramafic rocks.

The highest concentrations of *yttrium* (20-30 ppm, maximum 42 ppm) are present in the top 1-2 m of colluvium-alluvium (Appendix Q10/19), with a steady decrease with depth to <10 ppm in saprolite (10-15 ppm in QGI27, section 12350 mN).

Uranium abundances (Appendix Q10/17) are generally low with, as for Y, the highest concentrations (2-4 ppm) in the top 1-2 m of colluvium-alluvium. The palaeochannel mostly contains 1.3-2.0 ppm U, with similar, sporadic concentrations in felsic saprolite. The remaining saprolite contains <0.5 ppm U, except in MOWI63 (12100 mN), in which U contents are 2-3 ppm.

Thorium distributions (Appendix Q10/16), similar to those of U and Y, show a weak 'enrichment' at surface. Colluvial and palaeochannel sediments contain 7-14 ppm Th. Saprolite commonly contains 2-7 ppm on felsic rocks and <2 ppm on mafic-ultramafic rocks.

7.3 Dispersion in plan

There were insufficient data to investigate dispersion in plan at Stellar, as only one drill section was analysed. Reliable samples from the section orthogonal to it could not be obtained (see Section 3.2.2). The following discussion covers data from Quasar, firstly investigating and comparing the top of the basement with the interface above the basement and then examining dispersion in the palaeochannel sediments, the colluvium-alluvium and the lag.

7.3.1 Top of saprolite and the saprolite-colluvium interface

The weathered Archaean at Quasar was eroded, prior to deposition of the colluvium-alluvium, with little preservation of sub-surface laterite, so that anomalies in this stripped environment will present very small targets. Thus, it is essential to capitalise on any dispersion halos that there may have been retained or developed since burial. The following dispersion halos may be present:-

i) 'Lateritic' halos in remnants of ferruginous saprolite, mottled zone and lateritic duricrust or gravels at the top of the weathered basement. Such material could be mechanically dispersed in the base of the colluvium-alluvium.

ii) Halos formed in soils developed on the partly stripped profile, now possibly represented by or incorporated in, the base of the colluvium-alluvium.

iii) Halos formed during or after deposition of the colluvium-alluvium, chemically dispersed into the sediments or along the unconformity. Such dispersion could still be active.

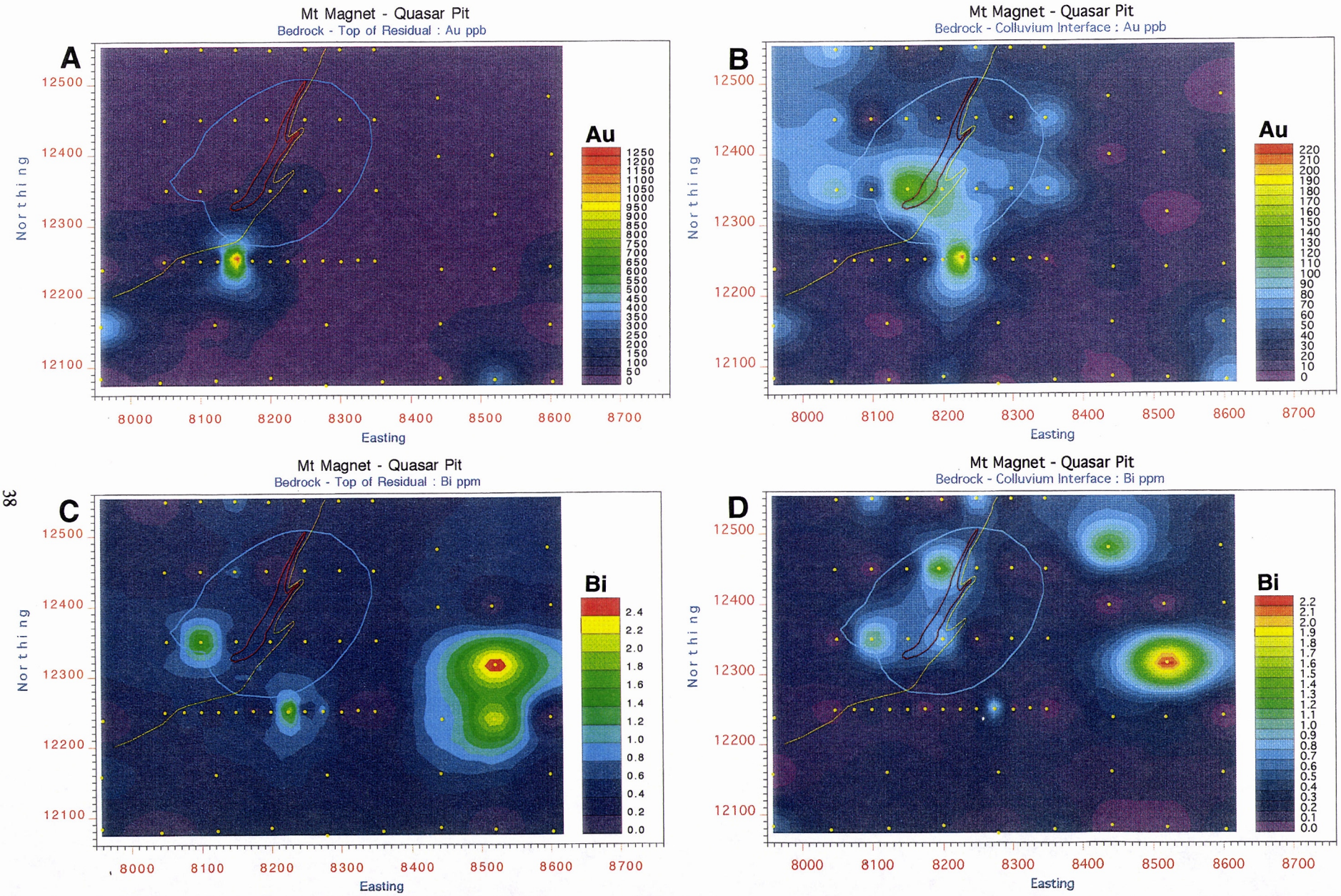

Figure 15. Comparison of distributions in top of residual profile and interface at base of colluvium for Au (A,B; ppb) and Bi (C,D; ppm) at Quasar. Note more diffuse but weaker, multipoint anomalies in interface sample compared to stronger, single-point anomalies in top of residuum.

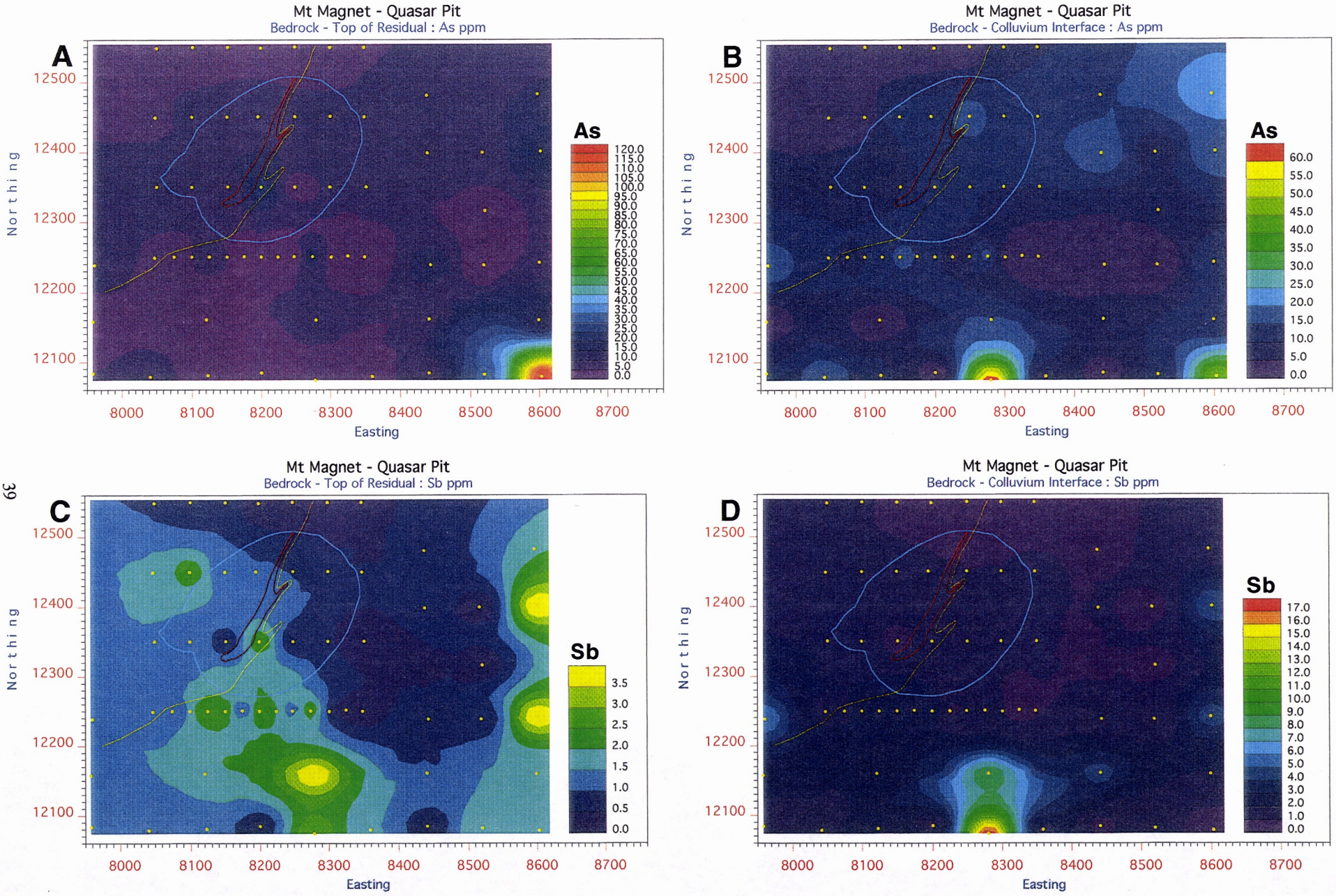

Figure 16. Comparison of distributions in top of residual profile and interface at base of colluvium for As (A,B) and Sb (C,D) in ppm at Quasar. Note very low As and Sb abundances in pit area but distinct anomalies on south and south-east.

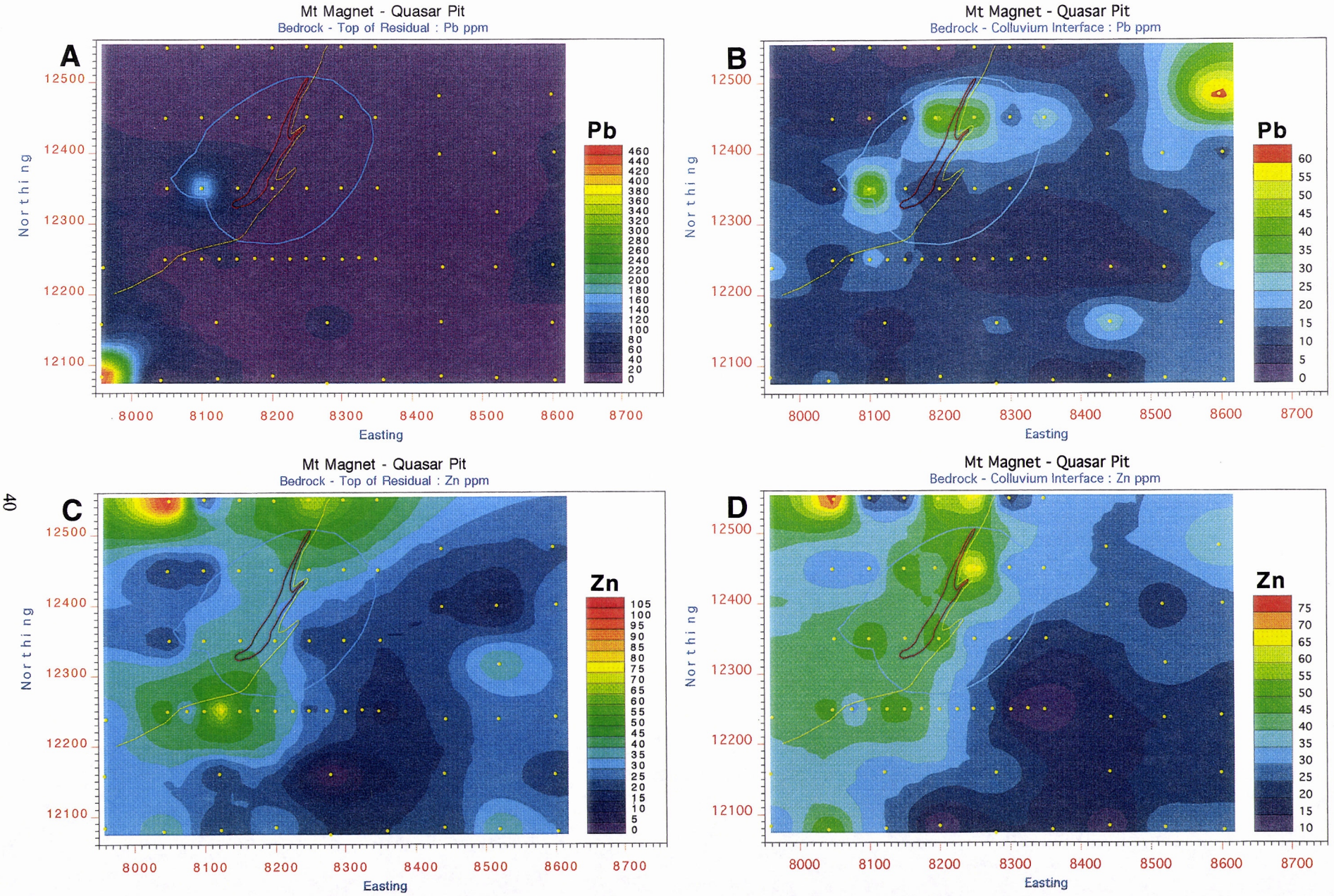

Figure 17. Comparison of distributions in top of residual profile and interface at base of colluvium for Pb (A,B) and Zn (C,D) in ppm at Quasar. Note moderate single point Pb anomaly in pit for top of residuum and more diffuse lower order anomaly for interface.

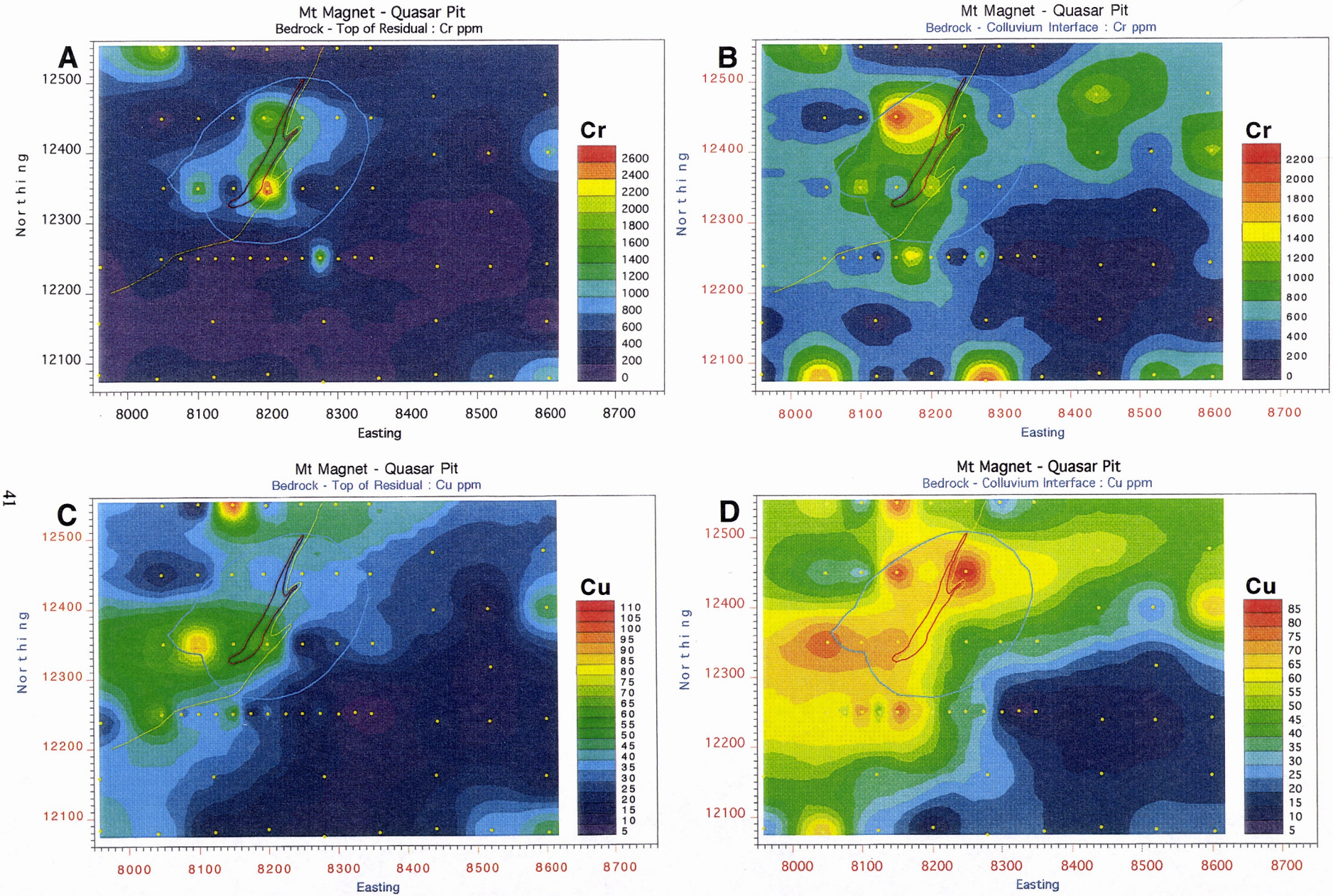

Figure 18. Comparison of distributions in top of residual profile and interface at base of colluvium for Cr (A,B) and Cu (C,D) in ppm at Quasar. Note greater concentrations in areas occupied by mafic-ultramafic rocks (north-west) compared to felsic rocks (south-east).

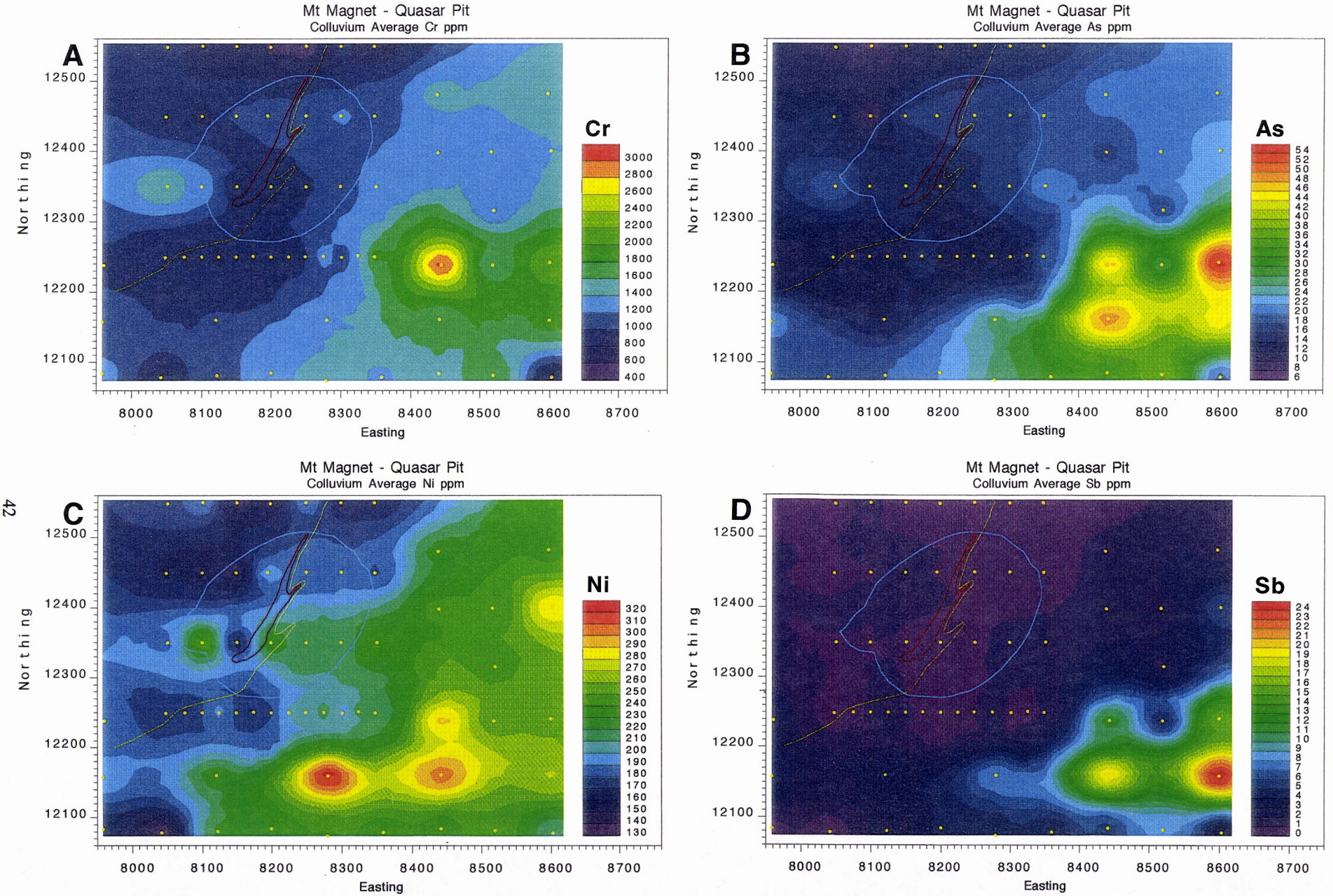

Figure 19. Comparison of distributions of Cr (A), Ni (C), As (B) and Sb (D) in mean colluvium in ppm at Quasar. Note similarity in distributions, apparently due to a shift in provenance of the detritus from mafic-ultramafic rocks in the south-east.

Accordingly, the most promising sample media were considered to be the upper metre of the residual regolith and the interface sample that includes the unconformity between weathered bedrock and the colluvium-alluvium. The latter would include contributions from each dispersion process. Where there was no specific interface sample, the two samples on either side of the interface, which would include the unconformity, were averaged. Data for these media are compared and presented in full in Appendix Q7, with critical maps in Figures 15-18. Data are given as part of Appendix Q1. Frequency distributions for these two sample media may be compared in Appendix Q9.

If the relationship of the drill pattern (yellow dots on Figures 15-19) to the outline of the mineralisation (red line on Figures 15-19) is examined, no drillholes have intersected the mineralisation at the levels examined. This is a very typical exploration situation. Reliance must then be placed on intersecting very minor mineralisation and dispersion halos.

Gold and lithologically-independent chalcophile pathfinder elements
Gold, in the top of the residual profile, gives a single point anomaly of 1460 ppb immediately south of the pit on the sheared contact (yellow line on Figure 15A). Less single point anomalies of 330-460 ppb occur to the south-west and south east of this. Adjacent drillholes have background abundances. There are no significant anomalies within the pit. While such a strong anomaly would doubtlessly be followed up, there is always a risk it may not have been as strong and, thus, may be given a much lower priority. In contrast, in the interface sample, there is a much broader, but lower order, anomaly of ~100 ppb, locally reaching 250 ppb, which occupies much of the southern part of the Quasar pit (Figure 15B).

Bismuth shows a localised concentration of >2.4 ppm to the east-southeast of the pit at the top of the residual profile (Figure 15C). Lesser anomalies (~1 ppm) occur at the south-west end of the pit and immediately to the south. Anomalies are of similar strength but are more widespread in the interface sampling over the western part of the pit (Figure 15D).

The *arsenic* and *antimony* contents of the primary mineralisation are very low and this is reflected by the absence of significant anomalies in either sample medium (Figures 16A-D). As observed in section, however, much higher concentrations of As (>120 ppm) and Sb (>17 ppm) occur to the east, suggesting a source east of the study area.. This is confirmed and better expressed in a plot of mean colluvium-alluvium abundances (Figure 19), described below. Arsenic and Sb are not effective in detecting Quasar-style mineralisation.

Lead shows a single point anomaly of 200 ppm at the top of the residual profile at the western side of the pit, coinciding with the Bi anomaly (Figure 17A, compare Figure 15C). Again, the interface sampling has broadened the target to an anomaly of 35-40 ppm in a background of 10 ppm, which overlies most of the northern part of the pit (Figure 17B).

Lithology-related elements
At the top of the residual profile, *chromium* shows increased abundances in the area of the pit and in the extreme north-west (Figure 18A). It also shows a generally increased abundance in the north and north east of the area, corresponding with the subcrop of mafic-ultramafic rocks, with a decreased abundance in the area generally occupied by felsic rocks. Very similar distributions are shown by *nickel, copper, vanadium and zinc* (Figures 17C and 18C). The interface samples have lower abundances of these elements (Figures 17D and 18D) but the dispersion patterns are more homogeneous and indicate the local lithological trend well.

Uranium and yttrium, particularly in the interface samples, depict a zone of higher abundances that approximately marks the sheared contact between the felsic and the mafic-ultramafic rocks. The abundances are very low and probably have little practical value.

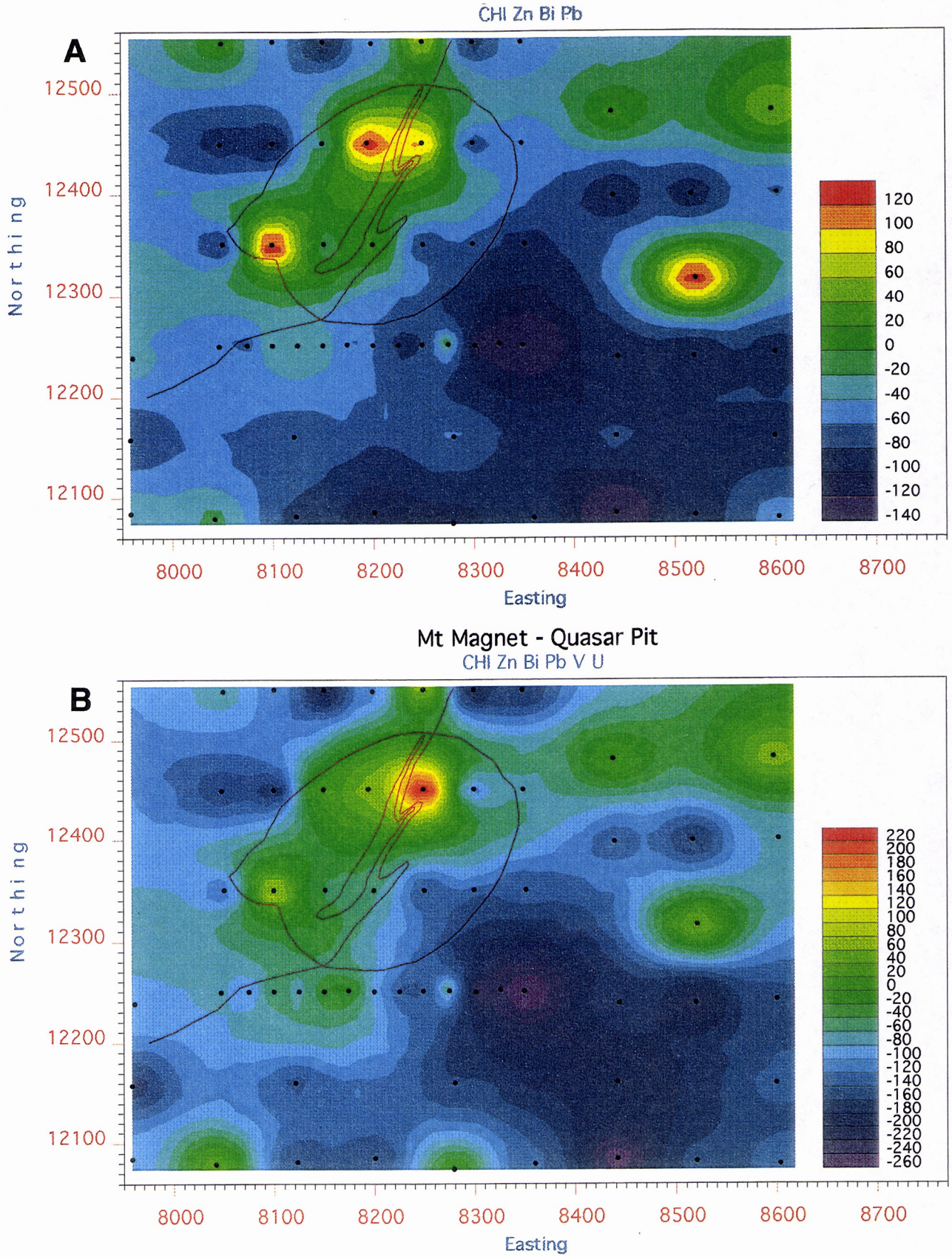

Figure 20. Additive indices using Bi, Pb and Zn (A) and Bi, Pb, U, V and Zn (B) for interface sampling at Quasar. Note improved targeting of mineralisation by using inter-element reinforcement of adjacent samples.

Multi-element index
A linear combination of pathfinder elements was investigated. Gold, which forms relatively small anomalies, was discarded for this exercise because i) a Au anomaly would be investigated exhaustively, ii) the distribution of Au data tends to be more intensely skewed than the other pathfinder elements.

A combination of Bi, Pb and Zn was investigated (Figure 20A), using interface sample data and this was later broadened (Figure 20B) to include U and V. Threshold abundances were subtracted and the remainder were scaled so that the ranges (above threshold) were approximately equal. These products were then summed as follows:-

i) CHI = 100(Bi-1) + 2(Pb-10) + 2.2(Zn-30)

ii) CHI = 100(Bi-1) + 2(Pb-10) + 2.2(Zn-30) +77(U-1.7) + 0.3(V-200)

After contouring, the results showed that such a combination of these pathfinder elements greatly improved the target size (above thresholds of 40 and 30 respectively) which accurately defined the mineralisation in the pit area. Apart from highlighting the multi-element nature of the geochemical halo, this additive technique allows neighbouring anomalies in different elements to reinforce one another, which is not achieved by processing single element data. Although the use of Bi-Pb-Zn alone highlighted another target, 270 m to the east of the pit, such an index has a more sound foundation than the one including U and V.

7.3.2 Palaeochannel sediments

Palaeochannel sediments, probably deposited in a fluvial or fluvio-lacustrine environment would be expected to have a detrital geochemistry related to their source rocks. However, adsorptive properties of the abundant clays in the sediments might contain post-depositional hydromorphic anomalies. Similarly, Fe-oxyhydroxides, in particular goethite, have very strong adsorptive properties for pathfinder elements and, where these have developed authigenically within the palaeochannel sediments, they could also inherit geochemical signals from a proximal basement source. Past groundwater flow directions (presumably dominantly along the palaeochannel) are critical to their interpretation.

Contoured plots of the arithmetic means of data from palaeochannel intersections are presented in Appendix Q8. The palaeochannel is restricted to the south-east of the study area; it is areally small and the data set comprises only 14 intersections incorporating 55 samples.

Statistical investigation of the individual palaeochannel samples shows several important correlations (Table 3). Arsenic is strongly correlated with Fe, Sb and Cr (Figures 21A, B, D). The strong As-Fe-Sb correlation indicates probable adsorption of As and Sb by Fe-oxides and suggests that the palaeochannel sediments, and particularly any authigenic ferruginous materials within them, may be useful regional prospecting media. The particularly strong correlation of Cr with Fe (Figure 21C) is typical of Fe oxides in the weathering environment and this explains the strong cross correlation of Cr with As. There are also correlations of Ba with Ga, Mn with Co, and Ni with Co (Table 3). Gold, as usual, shows low correlations with most other elements.

Comparison of the contoured averaged palaeochannel data (Appendix Q8) with the underlying horizons (the top of the Archaean and the interface; Appendix Q7) shows some coincidence of anomalies for As, Au, Ba, Bi and Ga, particularly between the mean palaeochannel and the top metre of the Archaean. The small area, small number of intersections and the very short course

TABLE 3
PALAEOCHANNEL SEDIMENTS AT QUASAR
SPEARMAN RANK CORRELATION - n=55

	As	Au	Ba	Bi	Co	Cr	Cu	Fe	Ga	Mn	Nb	Ni	Pb	Sb	Th	U	V	Y	Zn
As	1.00																		
Au	0.18	1.00																	
Ba	0.33	0.28	1.00																
Bi	0.06	0.05	0.25	1.00															
Co	0.29	-0.01	-0.08	-0.14	1.00														
Cr	0.68	0.23	0.39	-0.07	0.37	1.00													
Cu	0.64	0.35	0.26	-0.01	0.59	0.52	1.00												
Fe	0.77	0.25	0.51	-0.02	0.33	0.96	0.58	1.00											
Ga	0.41	0.44	0.68	0.29	-0.05	0.44	0.24	0.49	1.00										
Mn	0.38	0.11	0.16	-0.03	0.81	0.38	0.74	0.41	0.00	1.00									
Nb	0.34	0.11	0.03	-0.18	0.65	0.18	0.57	0.19	0.14	0.59	1.00								
Ni	0.40	0.02	-0.05	-0.20	0.87	0.52	0.58	0.46	0.08	0.64	0.66	1.00							
Pb	0.61	0.38	0.42	0.03	0.45	0.61	0.74	0.64	0.32	0.62	0.30	0.46	1.00						
Sb	0.76	0.12	0.38	0.14	-0.06	0.44	0.33	0.57	0.31	0.06	-0.04	0.06	0.45	1.00					
Th	0.71	0.32	0.39	-0.05	0.40	0.73	0.67	0.71	0.61	0.42	0.57	0.56	0.61	0.33	1.00				
U	0.36	-0.04	0.13	-0.39	0.23	0.48	0.11	0.44	0.29	0.08	0.20	0.44	0.21	0.22	0.50	1.00			
V	0.74	0.29	0.51	0.02	0.35	0.94	0.63	0.96	0.49	0.47	0.29	0.47	0.66	0.48	0.79	0.43	1.00		
Y	0.05	0.00	-0.26	-0.25	0.58	0.04	0.48	-0.04	-0.29	0.59	0.46	0.43	0.28	-0.23	0.15	-0.03	0.06	1.00	
Zn	0.26	0.27	0.19	0.05	0.64	0.43	0.56	0.39	0.36	0.62	0.63	0.62	0.44	-0.18	0.63	0.28	0.48	0.35	1.00

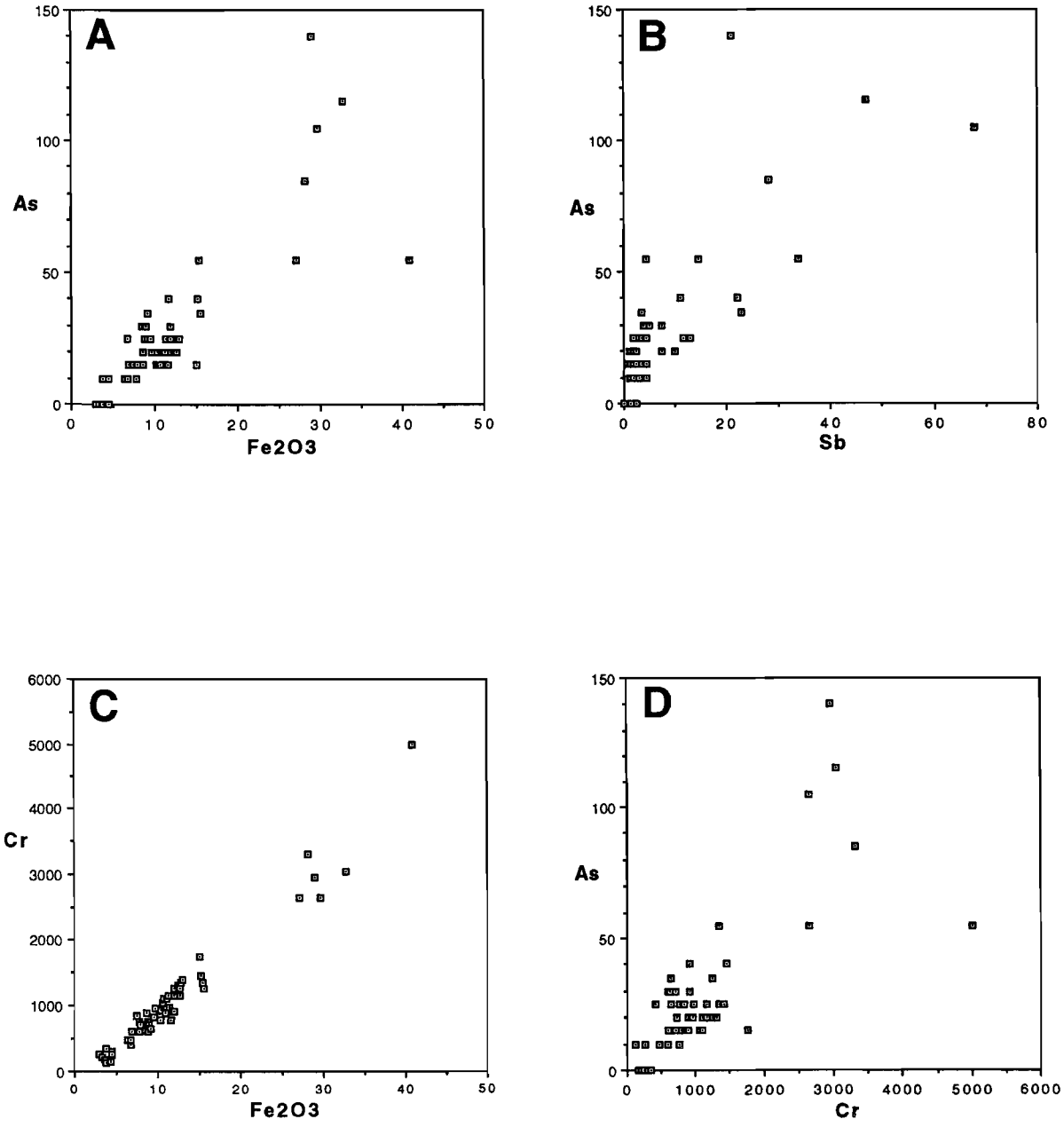

Figure 21. Well-correlated inter-relationships between metalloids As and Sb with Fe and Cr in palaeochannel sediments at Quasar.

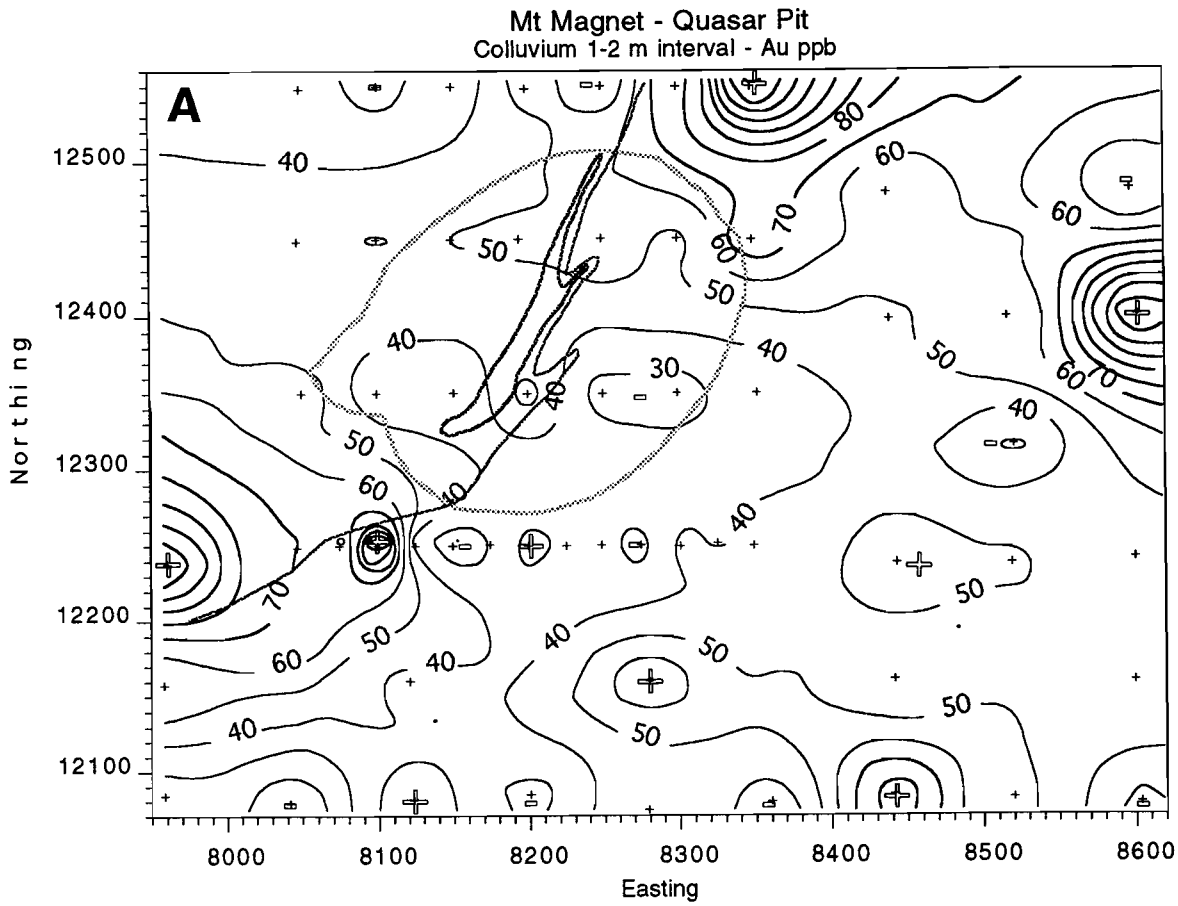

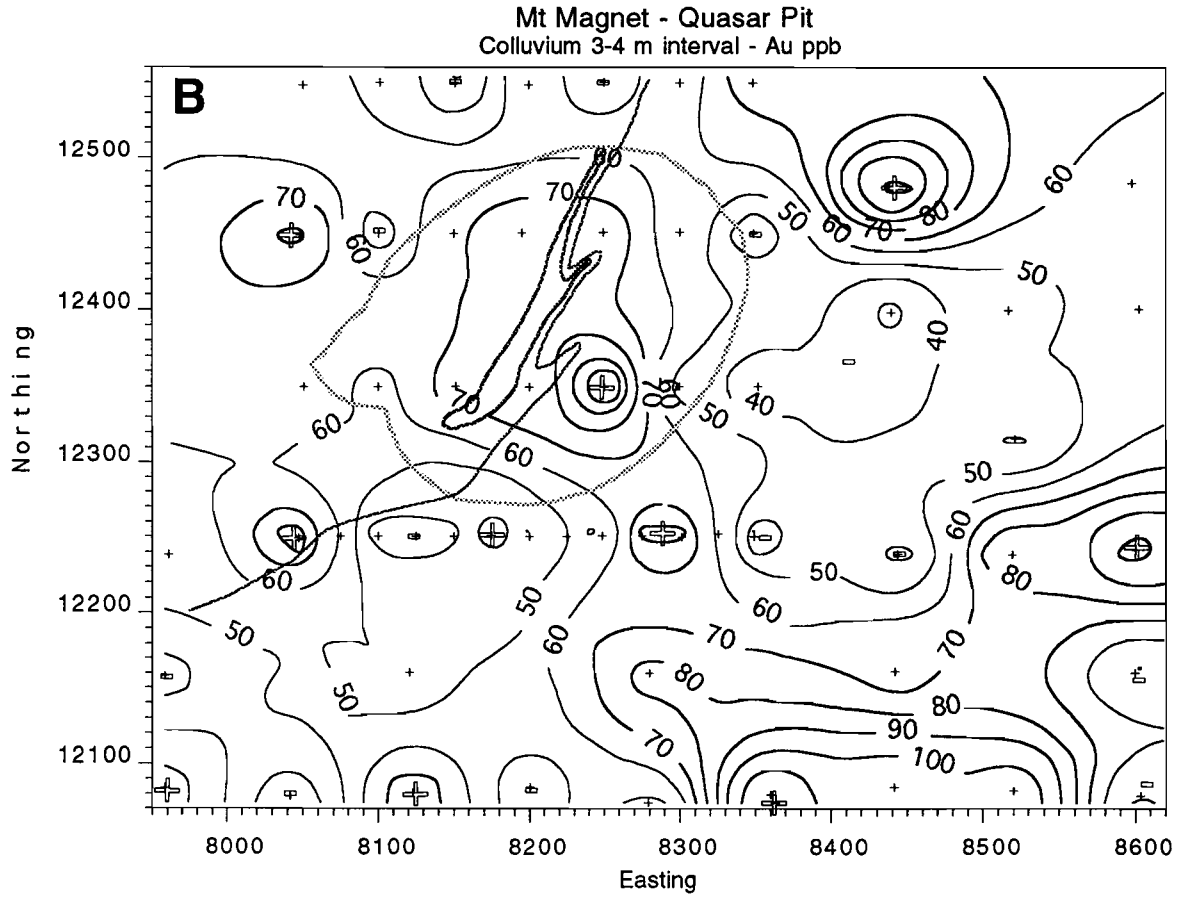

Figure 22. Comparison of Au distributions in 1-2 (A) and 3-4 (B) m intervals in colluvium at Quasar. Note lack of correlation between these almost adjacent units.

of the palaeochannel through the study area prevents anything but the most preliminary observations with the *caveat* that comparison of two very small, random, multi-element data sets may, co-incidentally, give similar results for some elements.

7.3.3 Colluvium-alluvium

The colluvial blanket, derived from the auriferous Boogardie Synform, has imported detritus with an apparently high Au background (mean ~50 ppb). The distribution of Au in this material will depend upon:-

i) The provenance of the detritus, noting that this may not remain constant during the period of deposition;

ii) The form of Au (i.e., micro-nuggets versus finely-divided or 'chemical' Au);

iii) The effects, if any, of chemical dispersion from underlying mineralisation.

Superimposed on this will be the practical effects and limitations of the sampling method, in this case aircore drilling.

Experience elsewhere has shown that the top metre and, in places, more than this, may be contaminated with material from the lowermost part of the previous drillhole. Consequently, as a precaution, the first metre was ignored.

The vertical compositional relationships between different units of the colluvium-alluvium and their consistency were investigated by contouring and comparing the Au data from the 1-2 m and 3-4 m intervals (Figures 22A and 22B). This showed that, although there are some locally high Au abundances (150 ppb) in both intervals, there is no reliable spatial correspondence between these two almost adjacent layers, nor with the basement. Similarly, the distributions in these layers have no correspondence to 'anomalies' in the overlying lag (Appendix Q6), indicating the latter to be false or 'rootless' anomalies (see Section 7.3.4). Further examination of this interlayer correlation for other elements showed very low correlations (Au r=0.068; Pb r=-0.006). For many elements (Au, Ba, Cu, Pb, Th, V) the correlations were less than the limit of 95% confidence (0.218) and should be regarded as probably random. Those that exceeded this limit are either related to lithology of provenance (Co, Cr, Fe, Ga, Nb, Ni) or to the depth of subsequent hardpanisation (Mn). The only pathfinder elements for which there was any significant interlayer correlation within the colluvium-alluvium were As and Sb (r=0.488 and 0.541 respectively) and these were investigated further.

The arithmetic mean composition of the colluvium-alluvium was computed (ignoring the top metre and the interface sample). Contoured data are presented in full in Appendix Q6 and critical geochemical maps in Figure 19. Plots of the mean As and Sb contents (Figures 19B, D) show strong concentrations in the south-east, peaking at 54 ppm As and 24 ppm Sb, in backgrounds of 20 ppm and 4 ppm, respectively. If these 'anomalies' are compared to the distributions of Cr and Ni, very similar patterns emerge (Figures 19A, D). These As and Sb anomalies in the colluvium-alluvium are partly underlain by basement and partly by palaeochannel sediment, which also contains As and Sb anomalies of similar abundances (compare Appendix Q6 with Q8). The data suggest derivation from a dominantly mafic-ultramafic source in the south-east. A much less likely possibility is that anomalies in the palaeochannel, which may or may not be proximally derived from the basement, have hydromorphically printed through into the colluvium-alluvium.

7.3.4 Lag

Lag has been used extensively by WMC as a prospecting medium (Carver *et al.*, 1987). It is particularly effective in areas of complete or stripped profiles in residual and erosional regimes where the geochemical signal is provided by chemically dispersed elements trapped in lateritic nodules and pisoliths and from mechanically dispersed gossan fragments (Robertson, 1989 and 1990). It is much less effective in depositional areas (Robertson and Wills, 1993); being dependent on bioturbation or churning to bring fragments to the surface and is unlikely to be effective where cover is more than one metre thick. As the colluvium-alluvium is not a good geochemical medium at Quasar, it would seem improbable that lag derived from it would be of much value either.

A suite of lag samples were collected by Hill 50 Gold Mine NL prior to mining but after extensive drilling and results are included in this orientation study. Data from a total of 127 lag samples (2-6 mm) are presented in tabulated form (Appendix Q4) and as histograms (Appendix Q5). Most of the data show approximately normal distributions (Fe, As Bi, Co, Cr, Cu, Ga, Nb, Ni, Sb, Th, U, V, Y and Zn), although a few are positively skewed (Au, Ba, Mn, Pb). The distributions of most elements (As, Ba, Co, Cr, Cu, Mn, Nb, Ni, Pb, Th, U, Y, Zn) are very spiky, consistent with randomly distributed data (Appendix Q6). The distributions of Fe, Sb and Bi are more consistent, suggesting Sb and Fe were derived from the east and south-east. These may reflect differing colluvial provenances. Comparison between geochemical distributions in the lag with those of deeper layers of the colluvium-alluvium and the top of the residuum shows that there is no relationship between the media. The lag is likely to have been derived from material similar to that occurring in the top 250-500 mm, but this was not investigated due to the possibility of contamination.

Nevertheless, there are some low-order Au lag anomalies over the pit. These may i) reflect the known Au anomaly in the saprolite, below the colluvium-alluvium, which has been transferred through the colluvium-alluvium to the lag, ii) represent random 'nuggety' high abundances derived from the auriferous provenance of the colluvium-alluvium and these 'spot' high abundances fall coincidentally close to the pit, iii) have resulted from contamination of the lag from nearby drilling. The first explanation is unlikely, in view of a lack of comparison between the lag and the mean colluvium-alluvium and its 1-2 and 3-4 m layers. Because the samples were not washed, contamination is the most likely, but there may be some 'nugget' influence.

7.4 Regolith discrimination

7.4.1 Stellar

A ternary Si-Al-Fe plot, with Fe corrected for analytical discrepancies (Section 3.6), is shown in Figure 23A. There is considerable overlap of the main regolith units on this diagram, showing that the major elements are not very effective in distinguishing between them There appear to be two saprolite groups. One is very Fe-poor, is clay-rich, of felsic origin and clusters close to the Si-Al axis. The other is more Fe-rich and of mafic-ultramafic origin. The duricrust is poorer in Fe and richer in Al than would normally be expected, reflecting its clay-rich nature, whereas the lateritic gravels, from which much of the clay has been lost, is more Fe rich than the duricrust. The colluvium-alluvium shows a linear trend from the Si-Al axis towards the Fe apex and is less Al-rich than the duricrust. The majority of the palaeochannel sediments are slightly poorer in Fe and richer in Al than the colluvium-alluvium.

A Cr-Fe binary plot (Figure 23D) clearly distinguishes between most residual materials (saprolite, clay saprolite, mottled zone, ferruginous saprolite, duricrust and lateritic gravel) and transported regolith materials (gravelly colluvium-alluvium, clay-rich colluvium-alluvium and palaeochannel sediment). There are minor overlaps between palaeochannel sediments and felsic saprolites, but the former tend to be more ferruginous.

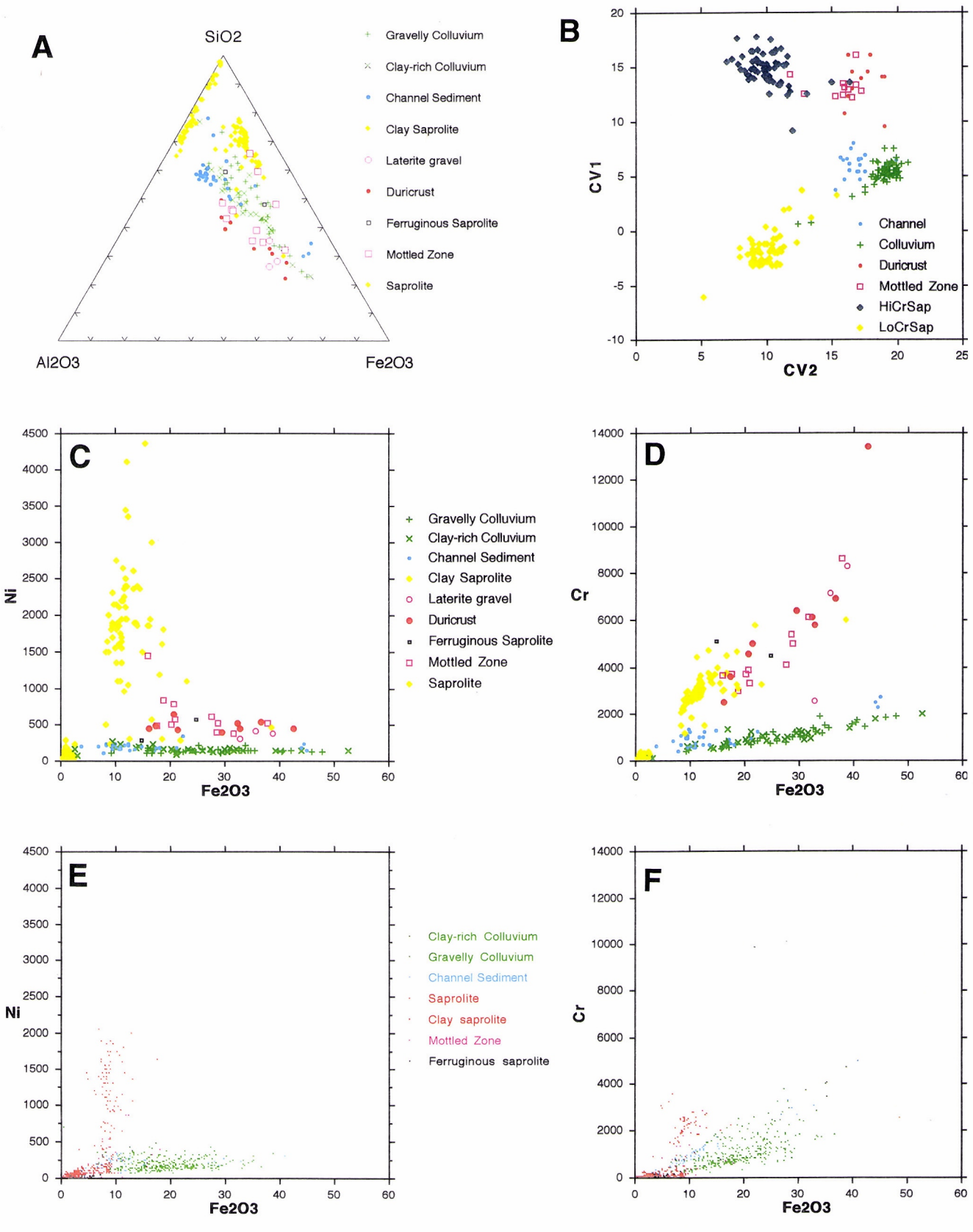

Figure 23. Regolith discrimination, at Stellar (A,B, C,D) and at Quasar (E.F).

The Ni-Fe plot (Figure 23C) produces similar results; one group of saprolites is particularly Ni- and Fe-rich, another Ni- and Fe-poor, corresponding to the mafic-ultramafic and felsic groups respectively. The separation between the Fe-rich residual materials and the transported materials is not great but there is little overlap.

Discriminant analysis was used to optimise the separation of regolith units. Separate databases of colluvium-alluvium (30 samples), palaeochannel sediment (66), duricrust (12), mottled zone (11) Cr-poor saprolite (67) and Cr-rich saprolite (64) were produced. Pathfinders Au, As and Sb were eliminated. The data distributions of each were examined and obvious outlying samples were removed. The remaining data were normalised; no transformations were needed for Si, Fe, Al and Ga, log transforms were applied to Co and Mn and power transforms were applied to the remainder. Canonical analysis produced a good separation (Figure 23B), although the mottled zone and duricrust are still mixed. Most of the discrimination is achieved by the first two canonical variates (CV1, CV2), with little useful information in CV3. The most useful elements appeared to be Al, Fe, Ni, Cr, Ga, Y, Zn, Th and Cu but not necessarily in that order.

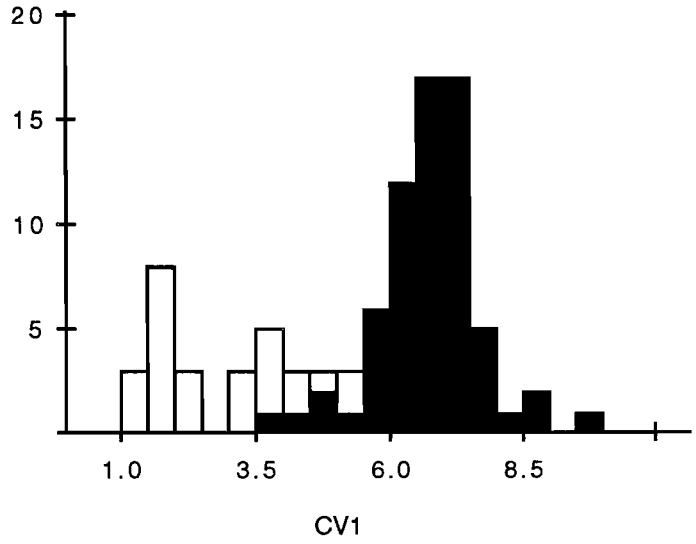

Figure 24. Bar chart of canonical analysis of colluvium (black) and palaeochannel sediments (white), giving overlapping populations. Stellar database, transported materials only.

Good discrimination between colluvium-alluvium and palaeochannel sediments was not possible when all the data were considered together. However, as the transported materials can be readily distinguished from the residual materials, a separate data set of transported materials only was prepared. Canonical analysis of the two groups yielded a single canonical variate, shown as a barchart (Figure 24). The more abundant colluvium-alluvium (black) overlaps slightly with the palaeochannel sediment (white). The histogram suggests that the palaeochannel sediment is polymodal in multivariate space. Most of the distinction is achieved by Fe, V, Y and U (Figure 25).

7.4.2 Quasar

It was not possible to plot a major element ternary diagram for Quasar as Al and Si had not been determined. However, very similar Cr-Fe relationships are found (compare Figure 23D with Figure 23F), although the lack of ferruginous residual material (duricrust, laterite gravel and mottled zone) limit the Cr variance. The transported materials (colluvium-alluvium and palaeochannel sediments) show their characteristic field of low Cr/Fe ratios, although the variance in this ratio is slightly greater, reflecting a more extensive data set and a more varied provenance. The saprolite shows two distinct fields, one with a high Cr content (mafic-ultramafic lithologies)

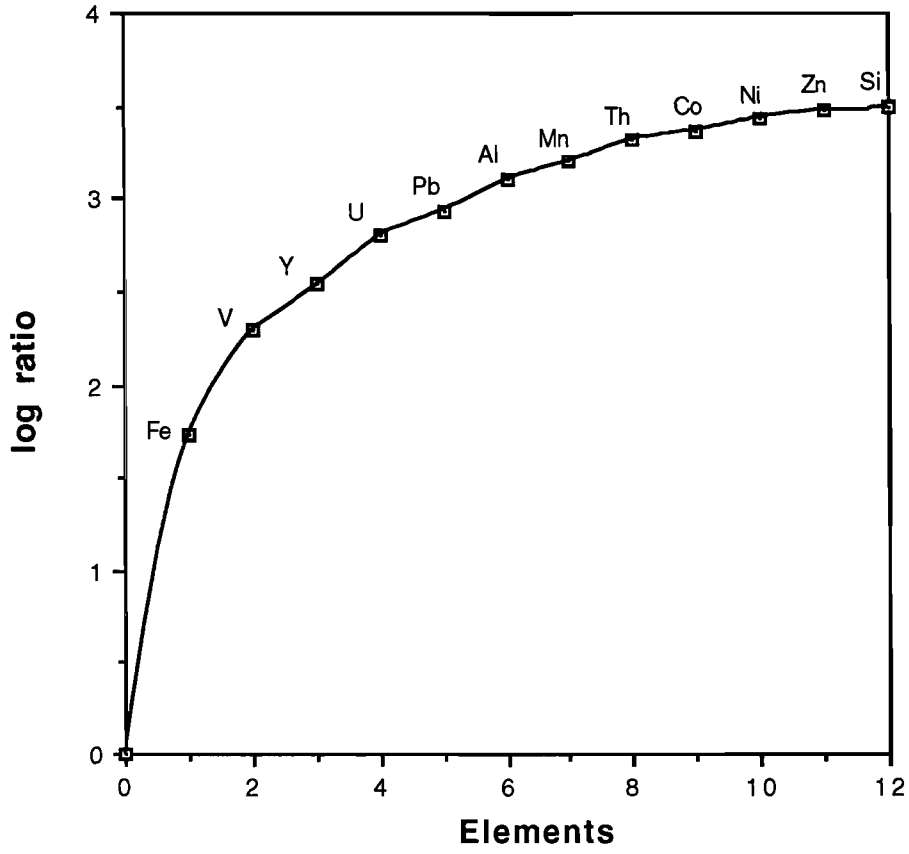

Figure 25. Efficacy of elements in canonical analysis of colluvium and palaeochannel sediment datasets. The most effective elements in making an imperfect distinction are Fe, V, Y and U. Stellar database, transported materials only.

and another with a low Cr content (felsic lithologies). Similar relationships to Stellar are apparent in the Ni-Fe relationships. As with Cr, the Ni variance is less for the residual materials and, although the absolute values in Ni and the Ni/Fe ratio are still low, their variances are slightly greater than at Stellar. Again, two saprolite fields are apparent, the Ni-rich corresponding with the Cr-rich fields.

8 SUMMARY AND CONCLUSIONS

Colluvium-alluvium covered plains, blanketing variably stripped lateritic terrain, such as those covering the Boogardie Synform at Mt Magnet, are one of several transported overburden covered environments being investigated by CSIRO-AMIRA project P409. This particular area is rendered more difficult for prospecting by a covering of detritus, derived from auriferous surroundings, and by numerous mineralised sites within the basement of the area, resulting in relatively high geochemical backgrounds. Beneath this cover is a network of palaeochannels, making the regolith stratigraphy complex and interpretation of dispersion patterns more difficult. Central to a correct exploration strategy are, firstly, a proper understanding of the subsurface regolith stratigraphy and, secondly, optimal choice of geochemical sample media and sampling density.

8.1 Regolith-landform evolution

8.1.1. Laterite

Differing relic fabrics in the lateritic nodules and pisoliths at Stellar demonstrate formation from mixed parent materials. These nodules and pisoliths were formed *in situ* in these clay-rich parent materials. The chemical composition of the underlying horizons (mottled clay zone and saprolite) seem related to the compositions of their parent rocks. Geochemical contrasts between parent lithologies (e.g., in Cr and Fe contents) diminish from the bottom to the top of the profile, but remain evident in the saprolite. However, in the lateritic duricrust, the Al, Si, Fe, Mg, Zr, Cr and Ni contents are very similar over both felsic and ultramafic rocks and suggest that the laterite has developed in transported material. Significant concentrations of Au and As occur in the laterite over both felsic and ultramafic rocks. Thus, the petrographic and geochemical evidence suggest that the lateritic profiles at Stellar are polygenetic. From this it is suggested that:-

i) Deep weathering has formed clay-rich saprolite above felsic and ultramafic bedrocks. Mass flow and/or erosion, during or after this event, led to development of a mixed surface horizon that formed the parent material of much of the laterite.

ii) Lateritisation during and after sedimentation developed nodules and pisoliths in this mixed, semi-residual to transported material, resulting in petrographic and geochemical homogeneity of the lateritic horizon above both ultramafic and felsic bedrocks. The laterite formed from vertical diffusion and local lateral movement of Fe in groundwater, followed by precipitation of Fe oxides in the upper profile. Gold, As, Cr and Ni were similarly dispersed hydromorphically during this phase.

Thus, it is suggested that the laterite at Stellar consists of allochthonous weathered material that was redistributed by water and later cemented. Gold was subsequently introduced from the adjacent mineralisation during lateritisation.

The presence of smectite, in the upper saprolite and laterite and of sepiolite in the palaeochannel and colluvium-alluvium at Stellar suggest weathering under conditions of restricted drainage. In contrast, kaolinite is formed under a strongly leaching, acidic environment. In lateritic environments, the presence of smectite is generally considered to be a late stage modification of

the regolith, related to a change to more arid conditions. The smectites may represent an intermediate stage in the weathering of primary silicates and persist due to the low degree of leaching. Smectite might also form from kaolinite, where the activities of $Si(OH)_4$ and alkaline earths are high, with excess Mg and Si precipitating as sepiolite.

8.1.2. Transported overburden

Palaeochannel sediments

The characteristics of these sediments indicate a complex history of deposition and modification by weathering. The palaeochannel at Stellar is similar to those described for many major drainages in the Kalgoorlie region, in which the sediments are considered to be late-Eocene (Anand *et al.*, 1993b; Kern and Commander, 1994) and were deeply weathered and lateritised after sedimentation. The considerable abundances of kaolinite represented by these sediments (the "Perkolilli Shale") were probably derived from the erosion of an existing regolith, suggesting that the landsurface may have already been deeply weathered prior to the Eocene. Further deep weathering of the channel sediments, and adjacent and underlying bedrock, then took place.

Such multiphase regolith development of the palaeochannels is evident at Stellar. The sediments contain hematite- and maghemite-rich ferruginous gravels, that appear to be detrital, transported with other clastic material, including quartz. The channel sediments and adjacent wall-rocks were then lateritised, with mega-mottles forming in the channel clays and hematitic and goethitic pisoliths and nodules forming over both felsic and ultramafic rocks.

The detrital origin of at least some of the gravels in the palaeochannels is suggested by differences in their location in the regolith profile, their mineralogy and their low Au and As contents compared to the nodules and pisoliths of the duricrust. The gravels were presumably derived by erosion of an earlier, possibly pre-Eocene, laterite profile that predates incision of the palaeodrainage. However, more work is needed to confirm the existence and significance of this earlier phase of weathering.

At both Quasar and Stellar, the morphologies (Figures 5A and 14A) suggest bowed fluvial channels, with the deepest incision and a steeper bank on the outside of the bend and a gentle slope and lesser incision (due to lower water velocities) on the inside. Logging of the extensive drilling in this region could be used to map out these palaeochannels; accurately locating these palaeochannels will be essential in interpreting the geochemistry.

Colluvial-alluvial sediments (Quaternary)

The colluvial-alluvial cover over the area has been derived from the dismantling of the lateritic regolith. The sediments are rich in ferruginous nodules and pisoliths, some possibly proximal to the lateritic source. Most, however, are polymictic and include fragments of BIF, ferruginous saprolite, saprolite and saprock as well as lateritic debris, and are probably distal from their source. The silty-clay matrix is largely derived from saprolite. The upper two to three metres of colluvial-alluvial sediments have been silicified, to form red-brown hardpan. In general, in the lower parts of the cover, the sedimentary environment tended to be alluvial and in the upper parts, the environment tended to be colluvial, probably dominated by sheet wash.

8.2 Three dimensional regolith modeling

Regolith logging of drill cuttings at Stellar and Quasar and contouring the thicknesses and lower surfaces of transported components have proved useful in depicting the regolith in three dimensions (Figures 5 and 14). These have assisted in developing an understanding of regolith history, palaeogeography and dispersion patterns.

8.3 Geochemistry

8.3.1 Geochemical data verification

Comparisons with reliable total analytical methods (XRF and INAA) indicated that ICP analysis, after a triple acid ($HF/HNO_3/HClO_4$) digest, produced results of questionable quality for a few of the elements, particularly for Ti and Zr. Molybdenum and calcium data were also unreliable at low concentrations and Fe and Cr were consistently underestimated. Although giving an essentially "total" analysis of elements and materials, the mixed acid digestion is only partial, and inconsistently so, for elements hosted mainly in resistant, refractory minerals such as zircon, Ti oxides and spinels. Because of their unreliability, the Ti and Zr data were discarded. These elements are important for identifying the parent lithology of the regolith and their absence weakens the discrimination that has been possible. Particular care, therefore, is essential in the choice of analytical methods involving chemical dissolution and the use of data for which reliability is unknown. Inclusion of 'in house' weathered rock standards in the analytical chain is highly recommended. Reliable compositions of these need to be pre-determined for a wide suite of elements by replicate analysis by outside laboratories. Results for those elements for which the data are unreliable should, preferably, not be made available.

8.3.2 Geochemical backgrounds and thresholds

The geochemical background for Au in the colluvium-alluvium is generally high, apparently due to its derivation from auriferous source rocks. Because of the highly mineralised nature of the bedrock, backgrounds and thresholds must be regarded as local.

8.3.3 Pathfinder elements

The mineralisation at both Stellar and Quasar is characteristically poor in As and Sb and the only possible pathfinder elements, other than Au, are Pb and Bi. The role of Zn is uncertain; W was not determined. However, none of these, on their own, give a dispersion pattern that is particularly clearly related to the known mineralisation. It must be emphasised that other styles of mineralisation, with different geochemical signatures, may occur. Thus, the As-Sb anomalies, south-east of Quasar, may be significant indicators of a different style of deposit.

8.3.4 Geochemical distinction of regolith units and bedrock lithology

At Stellar, most regolith components may be separated, using a Cr-Fe plot. Residual and semi-residual components of the regolith (saprolite, ferruginous saprolite, mottled zone, clay-rich duricrust and lateritic gravel) have greater Cr/Fe ratios than transported components (colluvium-alluvium and palaeochannel sediment), although there is some overlap between sediments and Cr- and Fe-poor felsic saprolites. The colluvium-alluvium and palaeochannel sediments occupy overlapping fields. Similar results were obtained at Quasar, with a much larger data set, indicating that this distinction may have use throughout the Boogardie Synform.

Elevated concentrations of Cr, Ni, Cu, V and, possibly, Zn indicate mafic-ultramafic rocks. The absence of reliable Ti and Zr data somewhat limits confidence in the discrimination. The sheared contact between mafic-ultramafic and felsic rocks at Quasar appears to be indicated by weakly increased abundances of U and Y.

Differentiation can be improved by canonical analysis, where the felsic and mafic-ultramafic saprolites are well separated. The most useful elements appear to be Al, Fe, Ni, Cr, Ga, Y, Zn, Th and Cu. The fields of the colluvium-alluvium and palaeochannel sediments again overlap. A slight improvement is possible, using training sets of the transported materials alone. With these limitations, most of the distinction was provided by Fe, V, Y and U.

Multi-element geochemical differentiation of regolith should not be used as a substitute for proper logging of drill-cuttings but it could be used where original materials are no longer available and only pulps have been kept. Geochemical techniques for weathered rock type

distinction were discussed by Robertson and Butt (1993), where their localised value was emphasised and this, no doubt, applies here.

8.3.5 Top of basement sampling

Very persistent and closely-spaced bedrock sampling must be credited for past exploration successes in this colluvium-covered area. However, dispersion into stripped saprolite is minimal, requiring a closely spaced drill grid, and drilling deep into the saprolite is costly. Sampling of the top of the basement will include any remnants of ferruginous materials (laterite, ferruginous saprolite, mottled zone) but, although the elemental concentrations and anomaly/background contrasts in this environment are greater than in the overlying interface sampling, the anomaly sizes are small and chances of intersecting them are significantly reduced.

Small, single point anomalies on a 50 x 100 m drill grid for Au, Pb and Bi indicate the general position of mineralisation at Quasar. Ridge-like anomalies in Zn and Cu may indicate mineralisation but more probably indicate the mafic-felsic contact. There were no significant anomalies in As and Sb associated with Quasar-style mineralisation.

8.3.6 Interface sampling

The saprolite-colluvium interface may incorporate a residual or partly transported palaeosol, with greater scope for mechanical and hydromorphic dispersion, during and after sedimentation. Experience at Quasar has shown that, although the anomalies are of lower contrast (compare Figures 26A and B), their sizes are significantly greater than those of the top of basement samples. Multipoint anomalies in Au, Pb and Bi, on a 50 x 100 m drill grid, overlie the southern, northern and central parts of the Quasar pit site, respectively.

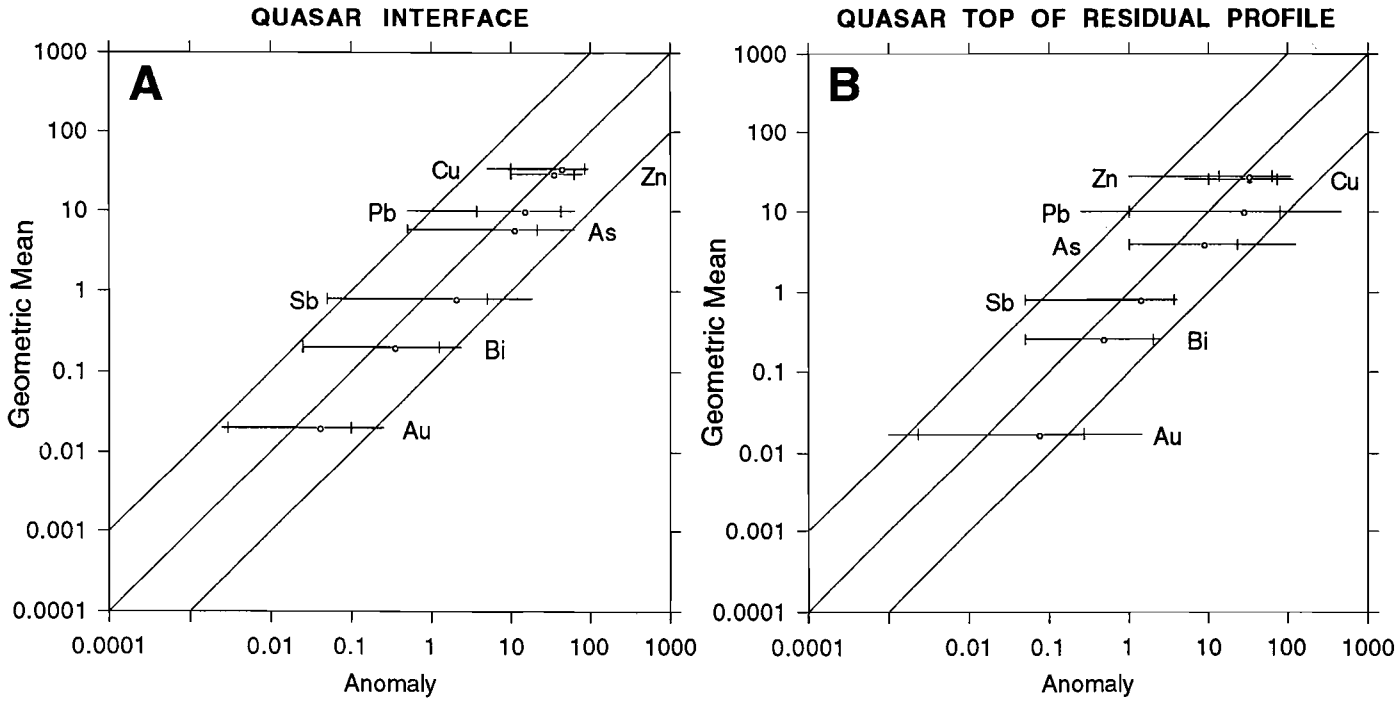

Figure 26. Log-log anomaly characterisation diagrams of interface (A) and top of residual profile (B) at Quasar showing greater anomaly contrast in residual material.

Although the interface sample is the preferred medium, there are circumstances where it may be less effective. In particular, where the basement is covered by a palaeochannel, the value of the interface samples either at the base of the colluvium-alluvium or at the base of the palaeochannel is questionable. However, authigenic Fe-oxides in the palaeochannel sediments may be useful geochemical media (see below).

8.3.7 Palaeochannel sediment

The fluvial environment of the palaeochannel implies that the geochemistry of any detrital materials are largely related to their distal source rocks. However, some of the ferruginous granules and mottles, within the palaeochannel at Stellar, appear to be authigenic (Section 6.1.2) and *may* have retained hydromorphic geochemical signals from proximal basement sources. The amount of palaeochannel available for detailed study at Quasar was too small to evaluate properly. However, the strong correlations of As and Sb with Fe makes this a possibility; the locally high As and Sb abundances suggest that dispersion of these metalloids in authigenic, ferruginous materials of the palaeochannels has potential for regional prospecting for As- and Sb-rich mineralisation.

8.3.8 Colluvium-alluvium

It is difficult to determine to what extent the low-order Au anomalies in the colluvium-alluvium are due to the presence of particulate Au, derived from the auriferous surroundings, or due to contamination during drilling; it is suspected that they are due to both. The significance of the Au distribution in the colluvium-alluvium is uncertain, but appears to be unrelated to mineralisation. There is little correlation between nearly adjacent layers in the colluvium-alluvium and there is no, specific source in the basement. If, as it seems at present, the colluvium-alluvium is ineffective as a sampling medium, it must be penetrated to sample the deeply weathered Archaean beneath.

8.3.9 Lag

The composition of the lag might be expected to reflect that of the uppermost layer of the colluvium-alluvium, from which it was probably derived. Detailed lag geochemistry was used in an area of generally thin (<1 m) colluvium at Bottle Creek (Robertson and Wills, 1982) with partial success, due to bioturbation within the colluvium bringing coarse components of the upper residual horizon to the surface. At Quasar, however, there is no satisfactory comparison between the compositions of the lag and the mean composition of the underlying colluvium-alluvium. This implies that there has been no significant bioturbation or churning of the colluvium, as suggested by the preservation of its layered structure. Thus, lag sampling appears to be inappropriate for exploration of areas having thick, colluvial cover, such as the Boogardie Synform.

8.4 Implications for Exploration

i) Probing for regolith stratigraphy, subsurface facies variations, presence of unconformities and the characteristics of buried erosional surfaces are important aspects of exploring areas of transported overburden and in deciding which units to sample. This requires care and time. Once the regolith stratigraphy is properly established, routine logging is much more efficient and relevant to data interpretation.

ii) It is necessary to detect and then determine the extent of areas where the complete or nearly complete laterite profile is preserved. Here, wide-spaced sampling, (500 m) of ferruginous materials from the top of the residuum is possible for regional exploration, given a suitable hydromorphic environment. Similarly, areas where the weathering profile is partly or extensively truncated should also be delineated. Here, dispersion is greatly restricted and

drill spacings, dictated by the expected target size, must be much closer (~50-100 m or less).

iii) Adequate regolith logging of drill cuttings is absolutely essential in areas covered by transported overburden to ensure the optimum sample medium is selected. A sample collected a metre too high could be in transported overburden, giving misleading results, whereas sampling too deep could include saprolite depleted in Au and pathfinder elements.

iv) Apart from Au, pathfinders for As- and Sb-poor Stellar and Quasar style mineralisation are limited to Pb and Bi, *possibly* with some input from Zn. However, none of these elements is an unequivocal guide to mineralisation.

v) Use of 'top of basement' sampling on a 100 x 50 m drill grid seems barely adequate for detection of a target such as Quasar. Use of 'interface' sampling gave a more certain result with this drill spacing. This is the preferred medium in areas of buried, truncated regolith. Logging of the extensive drilling in this region should be used to map out the palaeochannels as a guide to indicating areas where interface sampling is inadequate and as an aid for data interpretation.

vi) Improved target sizes and reduction of spurious anomalies were obtained using a multi-element index of the form CHI = 100(Bi-1) + 2(Pb-10) + 2.2(Zn-30). Gold could be included in this index or, at least, compared with it, for ranking anomalies for follow up. The use of this index needs further testing and improvement.

8.5 Recommendations for further research

i) Investigation of the geochemistry of the palaeochannels was inconclusive. The presence of authigenic Fe-oxides and the distributions of As and Sb are encouraging and suggest that specific analysis of authigenic materials may be used for regional prospecting. Authigenic mottles and ferruginous granules in the "deep leads" at Kanowna have anomalous As, Sb, W and Au concentrations (Anand *et al.*, 1993b), although this is not a feature of all such deposits. Use of these authigenic ferruginous materials needs to be investigated systematically and compared to more conventional methods. Regolith logging in the Boogardie Synform should define sites suitable for research into dispersion within palaeochannels from known mineralisation.

ii) The high background Au contents of the colluvium masks any hydromorphically-introduced Au derived from underlying mineralisation. Accordingly, the use of selective extraction analyses to investigate the distribution of labile Au may reveal significant low-order Au dispersion patterns having this origin. Such investigations are an important aspect of AMIRA Project 409 and are being undertaken at several locations. Experience has shown, however, that samples have to be collected specifically for this purpose, by shallow drilling. Cross-contamination is inevitable where deep drilling intersects bedrock mineralisation. Complete confidence in the sampling procedure is essential beforehand.

iv) The use of multi-element indices to broaden targets and reduce spurious anomalies (to assist with anomaly prioritisation) needs further evaluation. In particular, the distribution of W and, perhaps, Bi and Mo at lower detection limits, needs to be determined.

9 ACKNOWLEDGEMENTS

Assistance at Mt Magnet was provided by J. Block, M. Doyle, E. Faust and particularly by A.P Bristow and H. Warren. Thin and polished sections were prepared by R.J. Bilz and Ian Pontifex. Geochemical analyses were by WMC Exploration Division Laboratories at Kalgoorlie and by M.K.W. Hart (XRF) at CSIRO, Analabs (ICPMS) in Perth and Becquerel Laboratories (INAA) at Lucas Heights. X-ray diffraction analysis was by M.K.W. Hart and S.L. Derriman; interpretation was by C. Phang. Artwork was prepared by A.D. Vartesi and C. R. Steel. Technical assistance was by W.L. Maxwell and M.I. Svensson. V. M. Baker and R. Lee assisted with document formatting. All this assistance is acknowledged with appreciation.

10 REFERENCES

Anand, R.R., Churchward,H.M., Smith, R.E., Smith, K., Gozzard, J.R., Craig, M.J. and Munday, T.M. 1993a. Classification and atlas of regolith-mapping units-Exploration perspectives for the Yilgarn Craton. CSIRO Division of Exploration and Mining Restricted Report, 440 R, Unpaginated.

Anand, R.R., Smith, R.E., Phang, C., Wildman, J.E., Robertson, I.D.M and Munday, T.J. 1993b. Geochemical exploration in complex lateritic environments of the Yilgarn Craton, Western Australia. CSIRO Division of Exploration and Mining Restricted Report, 442R, 295 pp.

Archibald, N. 1982. Structure, lithological association units and gold mineralization, Mt Magnet area. in Archaean Geology of the Southern Murchison (Ed. J.L. Baxter), pp15-27. Geological Society of Australia, Western Australian Division: Perth.

Balde, R. and Woolfe, T.I. 1990. Saint George gold deposit, Mount Magnet, in Geology of the mineral deposits of Australia and Papua New Guinea (ed. F.E. Hughes). The Australasian Institute of Mining and Metallurgy, Melbourne. 255-258.

Butt, C.R.M., and Smith, R.E., (eds). 1980. Conceptual models in exploration geochemistry, 4 Australia. Developments in economic geology, 13. Elsevier, Amsterdam, 275 pp. (also Journal of Geochemical Exploration 12: 89-365).

Butt, C.R.M., Horwitz, R.C.H. and Mann, A.W. 1977. Uranium occurrences in calcretes and associated sediments in Western Australia, Report FP16. CSIRO Australia, Division of Mineralogy, Perth, 67pp.

Carver R.N., Chenoweth, L.M., Mazzucchelli, R.H., Oates, C.J. and Robins, T.W. 1987. "Lag" - A geochemical sampling medium for arid regions. Journal of Geochemical Exploration. 28: 183-199.

Gatehouse, S. 1989. Geochemistry of DDHs 5A, 8, 9, Milky Way and Stellar Prospects, Mt. Magnet, W.A. R.G.C Exploration Internal Report (Unpubl.).

Kern, A. M. and Commander, D.P. 1994. Cainozoic stratigraphy in the Roe Palaeodrainage of the Kalgoorlie region, Western Australia. In: Professional Papers: Western Australia Geological Survey, Report 34, 85-95.

Marjoribanks, R.W. 1989. Lithological, structural and regional setting of the Milky Way, Stellar and Andromeda Gold Deposits at Mount Magnet, W.A. R.G.C Exploration Internal Report (Unpubl.).

Perriam, R.P.A. 1990. The geology and gold mineralisation of the Mount Magnet Greenstone Belt. Western Mining Corporation Internal Report No: K-3253 (Unpubl.).

Robertson, I.D.M. 1989. Geochemistry, petrography and mineralogy of ferruginous lag overlying the Beasley Creek Gold Mine - Laverton, WA. CSIRO Division of Exploration Geoscience Restricted Report 27R. 181pp.

Robertson, I.D.M. 1990. Mineralogy and geochemistry of soils overlying the Beasley Creek Gold Mine - Laverton, W.A. CSIRO Division of Exploration Geoscience Restricted Report 105R. 158pp.

Robertson, I.D.M. and Butt, C.R.M. 1993. Atlas of weathered rocks. CSIRO Division of Exploration Geoscience Restricted Report 390R.

Robertson, I.D.M., and Wills, R. 1993. Petrology and geochemistry of surface materials overlying the Bottle Creek Gold Mine, WA. CSIRO Division of Exploration and Mining Restricted Report 394R.

Rose, A.W., Hawkes, H.E., and Webb, J.S. 1981. Geochemistry in Mineral Exploration. Academic Press. 657 pp.

Singer, A. 1979. Palygorskite in sediments: Detrital, diagenetic or neoformed - A critical review. Geol. Rundsch. 68: 996-1008.

Thompson, M.J., Watchorn, R.B., Bonwick, C.M., Frewin, M.O., Goodgame, V.R., Pyle, M.J. and MacGeehan, P.J. 1990. Gold deposits of the Hill 50 Gold Mine NL at Mount Magnet. in Geology of the mineral deposits of Australia and Papua New Guinea (ed. F.E. Hughes). The Australasian Institute of Mining and Metallurgy, Melbourne. 221-241.

Vann, J. 1989. Mount Magnet Project - Status report to July 1989. R.G.C. Exploration Pty. Ltd. Internal Report (Unpubl.).

Watkins K.P., and Hickman, A.H. 1990. Geological evolution and mineralization of the Murchison Province, Western Australia. Geological Survey of WA Bull 137.